Doping driven small-to-large Fermi surface transition and d-wave superconductivity in a two-dimensional Kondo lattice

R. Eder[1] and P. Wróbel[2]

[1]*Karlsruhe Institut of Technology, Institut für Festkörperphysik, DE-76021 Karlsruhe, Germany*
[2]*Institute for Low Temperature and Structure Research, P.O. Box 1410, PL-50-950 Wrocław 2, Poland*

We study the two-dimensional Kondo lattice model with an additional Heisenberg exchange between localized spins. In a first step, we use mean-field theory with two order parameters. The first order parameter is a complex pairing amplitude between conduction electrons and localized spins that describes condensation of Kondo (or Zhang-Rice) singlets. A nonvanishing value implies that the localized spins contribute to the Fermi surface volume. The second-order parameter describes singlet pairing between the localized spins and competes with the Kondo-pairing order parameter. Reduction of the carrier density in the conduction band reduces the energy gain due to the formation of the large Fermi surface and induces a phase transition to a state with strong singlet correlations between the localized spins and a Fermi surface that comprises only the conduction electrons. The model thus shows a doping driven change of its Fermi surface volume. At intermediate doping and low temperature, there is a phase where both order parameters coexist, which has a gapped large Fermi surface and $d_{x^2-y^2}$ superconductivity. The theory thus qualitatively reproduces the phase diagram of cuprate superconductors. In the second part of this paper, we show how the two phases with different Fermi surface volume emerge in a strong-coupling theory applicable in the limit of large Kondo exchange. The large Fermi surface phase corresponds to a "vacuum" of localized Kondo singlets with uniform phase, and the quasiparticles are spin-1/2 charge fluctuations around this fully paired state. In the small Fermi surface phase, the quasiparticles correspond to propagating Kondo singlets or triplets whereby the phase of a given Kondo singlet corresponds to its momentum. In this picture, a phase transition occurs for low filling of the conduction band as well.

I. INTRODUCTION

The existence and shape of the Fermi surface and its change with the hole concentration δ in the CuO_2 planes appears be one of the central issues in the physics of cuprate superconductors. In the overdoped compound $Tl_2Ba_2CuO_{6+x}$, magnetoresistance measurements,[1] angle-resolved photoemission spectroscopy (ARPES),[2] and quantum oscillation experiments[3] show a situation that is reminiscent of that in heavy fermion compounds: Despite the participation of the strongly correlated Cu3d orbitals in the states near the Fermi energy the Fermi surface agrees well with LDA band structure calculations, which take the Cu3d electrons as itinerant, quantum oscillation experiments show the validity of the Fermi liquid description with an enhanced band mass. The only moderate mass enhancement in the cuprates thereby seems natural given the large Cu3d-O2p exchange constant $W \approx 1$ eV, which would give a very high nominal Kondo temperature.

In the underdoped compounds, the situation is more involved. ARPES shows Fermi arcs[4] that, however, are probably just the visible part of hole pockets centered near $(\frac{\pi}{2}, \frac{\pi}{2})$. This is plausible because the sharp drop of the ARPES weight of the quasiparticle band upon crossing the noninteracting Fermi surface, which must be invoked to reconcile the Fermi arcs with the hole pocket scenario, is actually well established in insulating cuprates such as $Sr_2Cu_2O_2Cl_2$ (Ref. 5) and $Ca_2CuO_2Cl_2$,[6] where this phenomenon has been termed the remnant Fermi surface. Meng *et al.* reported the observation of the previously unresolved dark side of the hole pockets in underdoped $Bi_2(Sr_{2-x}La_x)CuO_6$ by ARPES.[7] Their conclusions subsequently were criticized[8] and the issue still seems controversial.[9]

Moreover, both the Drude weight in $La_{2-x}Sr_xCuO_4$ (Refs. 10 and 11) and $YBa_2Cu_3O_y$ (Ref. 11) as well as the inverse low-temperature Hall constant in $La_{2-x}Sr_xCuO_4$ (Refs. 11–14) and $YBa_2Cu_3O_y$ (Ref. 11) scale with δ and the inferred band mass is constant throughout the underdoped regime and, in fact, even the antiferromagnetic phase.[11] This is exactly the behavior expected for hole pockets. On the other hand, for $\delta \geqslant 0.15$, the Hall constant in $La_{2-x}Sr_xCuO_4$ changes rapidly, which suggests a change from hole pockets to a large Fermi surface.[12] Quantum-oscillation experiments on underdoped $YBa_2Cu_3O_{6.5}$ (Refs. 15–18) and $YBa_2Cu_4O_8$ (Refs. 19 and 20) show that the Fermi surface has a cross section that is comparable to $\delta/2$ rather than $(1-\delta)/2$ as in the overdoped compounds. Here, it should be noted that the mere validity of the Fermi liquid description as demonstrated by the quantum oscillations is conclusive evidence against the notion of Fermi arcs: The defining property of a Fermi liquid is the one-to-one correspondence of its low-lying states to those of a fictitious system of weakly interacting fermionic quasiparticles, and the Fermi surface of these quasiparticles is a constant energy contour of their dispersion and, therefore, necessarily a closed curve in **k** space. On the other hand, the quantum oscillations can not be viewed as evidence for hole pockets either in that both the Hall constant[21] and thermopower[22] have a sign that would indicate electron pockets. Thereby, both the Hall constant and the thermopower show a strong temperature dependence and, in fact, a sign change as a function of temperature. This sign change is observed only at temperatures where superconductivity is suppressed by a high magnetic field. At the same time, neutron scattering experiments on $YBa_2Cu_3O_{6.6}$ in the superconducting state

show pronounced anisotropy in the spin excitations spectrum below 30 meV and at low temperatures.[23] This indicates an as yet not fully understood anisotropic state, possibly to a nematic state with inequivalent x and y directions in the CuO_2 plane. Such a nematicity has also been observed in scanning tunneling microscopy experiments on $Bi_2Sr_2CaCu_2O_{8+\delta}$ (Ref. [24]) and will modify the Fermi surface in some way, which may explain the unexpected sign. More recently, Sebastian *et al.* concluded from an analysis of the second harmonic in quantum oscillations in underdoped $YBa_2Cu_3O_{6+x}$ that the Fermi surface consists only of a single pocket.[25] Since this would rule out the possibility of coexisting holelike and electronlike Fermi surface sheets,[26] and since it is hard to imagine that the sole Fermi surface sheet of a hole-doped compound is electronlike, this result would imply that the Fermi surface actually is a hole pocket and that the sign of the Hall constant and thermopower does not reflect the nature of the carriers but is determined by some other mechanism. By adopting this point of view, the picture of hole pockets centered near $(\frac{\pi}{2},\frac{\pi}{2})$ with an area $\propto \delta$ would give a simple and consistent description of ARPES, normal-state Drude weight and Hall constant, and quantum-oscillation experiments in the underdoped state. Combined with the results for the overdoped compounds, this would imply that as a function of δ the cuprates undergo a phase transition between two states with different Fermi surface volume, whereby the $Cu3d$ electrons contribute to the Fermi surface volume in the overdoped compounds but drop out of the Fermi surface volume in the underdoped regime.

Interestingly, the superconducting transition in the cuprates itself seems to be accompanied by a Fermi surface change as well. Namely, ARPES shows that the quasiparticle peaks near $(\pi,0)$, which are hardly distinguishable in the normal state, become very intense and sharp in the superconducting state.[27,28] This looks as if coherent quasiparticles around $(\pi,0)$ exist only in the superconducting state and, in fact, seem to jump into existence right at the superconducting transition.[29] A possible interpretation would be that the superconducting transition occurs between a hole-pocket-like Fermi surface, which does not extend toward $(\pi,0)$, to a gapped large Fermi surface, which naturally has some portions near $(\pi,0)$.

Transitions where the correlated electron subsystem contributes to the Fermi surface volume or not are not unfamiliar in heavy fermion compounds. An example is the metamagnetic transition in $CeRu_2Si_2$ where the Ce $4f$ electrons, which contribute to the Fermi surface in zero magnetic field, seem to drop out of the Fermi volume as the magnetic field is increased.[30] In $CeRh_{1-x}Co_xIn_5$, the Ce $4f$ electrons change from localized for $x \leqslant 0.40$ to itinerant for $x \geqslant 0.50$ as the lattice constant decreases due to substitution of Rh by the smaller Co.[31] Similarly, the localized Ce $4f$ electrons in $CeRh_2Si_2$,[32] $CeRhIn_5$,[33] and $CeIn_3$ (Ref. [34]) can be made itinerant by pressure. It seems that, in the case of the metamagnetic transition, the magnetic field breaks the Kondo singlets between Ce $4f$ spins and conduction electrons, whereas in the other cases, the decrease of the hybridization strength between $4f$ and conduction electrons makes the formation of Kondo singlets unfavorable.

It has been pointed out long ago by Doniach that there may be a competition between the Kondo effect and the Ruderman-Kittel-Kasuya-Yoshida (RKKY) interaction, which then leads to a phase transition to a magnetically ordered phase if certain parameters in the system are varied.[35] More recently, Senthil *et al.* have investigated this question in the context of heavy-fermion compounds and discussed a transition to a magnetically ordered state that is accompanied by a Fermi surface transition from large to small as the strength of the Kondo coupling is varied.[36]

In the cuprates, one might expect another reason for a Fermi surface transition, namely, the depletion of the mobile carriers, i.e., holes in $O2p$ orbitals. It is self-evident that the gain in energy due to formation of a common Fermi sea of mobile $O2p$ holes and localized $Cu3d$ spins must tend to zero when the density of mobile carriers vanishes. More precisely, one might expect the band filling to play a substantial role when the width of the occupied part of the conduction band becomes smaller than the width of the Kondo resonance at the Fermi level. Since the $Cu3d$-$O2p$ exchange constant is large and the band filling small, this situation may well be realized in the cuprates. As the density of holes in $O2p$ orbitals is reduced, one would thus expect that at some point the localized spins drop out of the Fermi surface so as to optimize their mutual superexchange energy instead. Due to the near two dimensionality of the cuprates, however, the transition is not to a magnetically ordered state, but to a spin liquid with strong nearest-neighbor singlet correlations instead of true antiferromagnetic order.

Cuprate superconductors are frequently described by a single-band Hubbard model or the t-J model. Whereas a Kondo-lattice-like Hamiltonian can be derived by lowest-order canonical perturbation model from the so-called d-p model for the CuO_2 plane,[37] these single-band models are obtained in a subsequent step, which is valid in the limit of large Kondo coupling between $O2p$ and $Cu3d$ electrons, so that the Kondo singlet (Zhang-Rice singlet) extends over little more than only one plaquette. Yet, these models should show a Fermi surface transition as well if they are equivalent to the CuO_2 plane. Exact diagonalization studies of the t-J model have indeed shown that the Fermi surface at hole dopings $\leqslant 15\%$ takes the form of hole pockets,[38–40] the quasiparticles have the character of strongly renormalized spin polarons throughout this doping range,[41–43] and the low-energy spectrum at these doping levels can be described as a Fermi liquid of spin-1/2 quasiparticles corresponding to the doped holes.[44] A comparison of the dynamical spin and density correlation function at low[45,46] ($\delta < 15\%$) and intermediate and high ($\delta = 30–50\%$) hole doping moreover indicates[47] that, around optimal doping, a phase transition to a state with large Fermi surface takes place in the t-J model. A study of the electronic self-energy in the single-band Hubbard model has indicated that such a transition takes place there as well.[48] Contrary to widespread belief, such hole pockets can be completely consistent with the Luttinger theorem for the single-band Hubbard model.[48]

To study the issue of the Fermi surface transition further, we performed a Hartree-Fock treatment of a two-dimensional Kondo lattice with an additional Heisenberg exchange between localized spins. This is presented in Sec. II. Interestingly, it turns out that such a transition not only exists but is generically accompanied by $d_{x^2-y^2}$ superconductivity in the mobile carrier system, which might provide an explanation for the phase diagram of the cuprates. In simplest terms, superconductivity

occurs because the coherent Kondo pairing between d spins and c electrons "transfers" the singlet pairing between the localized d spins to the mobile c-electron system.

Since a mean-field treatment may not really be expected to be valid in the limit of large superexchange W between localized and conduction electrons, which is the region of physical interest for the cuprates, we also show how the two phases with small and large Fermi surface may be understood in the limit of large W. The small Fermi surface phase is discussed in Sec. III and is similar to the lightly doped Mott insulator as discussed in Ref. 49. The phase with large Fermi surface is discussed in Sec. IV, closely following Refs. 50 and 51. Section V discusses the possibility of a phase transition between small and large Fermi surface within the strong-coupling theory, and Sec. VI gives a summary and discussion.

II. MEAN-FIELD THEORY

We study a Kondo lattice model that consists of a single metallic conduction band, described by the fermionic operators $c_{i,\sigma}^\dagger$, and a lattice of localized spins, described by $d_{i,\sigma}^\dagger$. The lattice sites, labeled by i, form a simple cubic lattice and there is one localized spin and one s-like conduction orbital in each unit cell. A similar model with two O$2p$-like conduction orbitals per unit cell can be derived by canonical transformation for the CuO$_2$ plane.[37] We augment the model by a direct Heisenberg exchange between nearest-neighbor localized spins. A similar model for the CuO$_2$ plane has been studied previously.[52] To make more easy contact with the CuO$_2$ planes, we consider the operators $c_{i,\sigma}^\dagger$ and $d_{i,\sigma}^\dagger$ to create holes rather than electrons. We denote the density of holes in the conduction band by δ; the total densisty of holes/unit cell thus is $1 + \delta$. The Hamiltonian reads as

$$
\begin{aligned}
H &= H_t + H_W + H_J, \\
H_t &= t \sum_{\langle i,j \rangle} \sum_\sigma c_{i,\sigma}^\dagger c_{j,\sigma}, \\
H_W &= W \sum_i \left(\vec{S}_{d,i} \cdot \vec{S}_{c,i} - \frac{n_{c,i} n_{d,i}}{4} \right), \\
H_J &= J \sum_{\langle i,j \rangle} \left(\vec{S}_{d,i} \cdot \vec{S}_{d,j} - \frac{n_{d,i} n_{d,j}}{4} \right),
\end{aligned}
\tag{1}
$$

where

$$
\begin{aligned}
\vec{S}_{c,i} &= \tfrac{1}{2} c_{i,\alpha}^\dagger \vec{\sigma}_{\alpha,\beta} c_{i,\beta}, \\
n_{c,i} &= c_{i,\alpha}^\dagger c_{i,\alpha},
\end{aligned}
\tag{2}
$$

with $\vec{\sigma}$ the vector of the Pauli matrices and analogous definitions hold for $\vec{S}_{d,i}$ and $n_{d,i}$. The model is to be considered in the sector of the Hilbert space where all d orbitals are singly occupied.

In a first step, we drop the d-d exchange H_J. We use the identity

$$
\begin{aligned}
\vec{S}_{d,j} \cdot \vec{S}_{c,j} - \frac{n_{d,j} n_{c,j}}{4} &= -\frac{1}{2} S_j^\dagger S_j, \\
S_j^\dagger &= c_{j,\uparrow}^\dagger d_{j,\downarrow}^\dagger - c_{j,\downarrow}^\dagger d_{j,\uparrow}^\dagger,
\end{aligned}
\tag{3}
$$

and apply the Hartee-Fock approximation

$$
S_j^\dagger S_j \approx \langle S_j^\dagger \rangle S_j + S_j^\dagger \langle S_j \rangle - \langle S_j^\dagger \rangle \langle S_j \rangle.
\tag{4}
$$

Whereas the original Hamiltonian conserves the number of d holes at each site, this does not hold true for the mean-field Hamiltonian, which is clearly a severe drawback of the theory. Although the present decoupling scheme is different from that used by Senthil *et al.*[36] the theories can be converted into each other in the case $J = 0$ by performing a particle-hole transformation for the d electrons.

There are two side conditions to be obeyed: one for the total hole number N_h, and the other one for the number of d holes N_d, which must be equal to N, the number of d sites in the system. We enforce these by Lagrange multipliers μ and λ, respectively, and, by introducing the vector $v_{\mathbf{k},\sigma}^\dagger = (c_{\mathbf{k},\sigma}^\dagger, d_{-\mathbf{k},\bar{\sigma}})$, we obtain the Fourier transformed Hamiltonian

$$
\begin{aligned}
&H - \mu N_h - \lambda N_d \\
&= \sum_{\mathbf{k},\sigma} v_{\mathbf{k},\sigma}^\dagger H_{\mathbf{k},\sigma} v_{\mathbf{k},\sigma} - 2N\epsilon_d + 2N\mu + N\frac{\Delta_{cd}^2}{2W},
\end{aligned}
\tag{5}
$$

where N_h (N_d) are the operators for the total number of holes (number of d-like holes), N is the number of sites, and

$$
\begin{aligned}
H_{\mathbf{k},\sigma} &= \begin{pmatrix} \epsilon_{\mathbf{k}} - \mu & -\text{sign}(\sigma)\frac{\Delta_{cd}}{2}, \\ -\text{sign}(\sigma)\frac{\Delta_{cd}}{2} & \epsilon_d - \mu \end{pmatrix}, \\
\Delta_{cd} &= W \langle S_j \rangle,
\end{aligned}
\tag{6}
$$

$$
\epsilon_d = \lambda + 2\mu.
\tag{7}
$$

The real parameter Δ_{cd} describes coherent singlet formation between the conduction electrons and the localized spins. The essence of the Kondo effect is the quenching of the magnetic moments, which means a localized spin at site i forms a singlet with a conduction electron (this would be the Zhang-Rice singlet in the case of cuprate superconductors). The phase of this local singlet then is, in principle, undetermined and the above mean-field decoupling describes a state where this phase is uniform over the whole system.

Next, being the expectation value of two creation and annihilation operators, Δ_{cd} has some similarity to a super-conducting order parameter. Since the pairing is not between time-reversed states, however, the resulting ground state is not superconducting. This will be apparent from the fact that it has a well-defined Fermi surface. The Hamiltonian can be diagonalized by the transformation

$$
\begin{aligned}
\gamma_{\mathbf{k},1,\sigma}^\dagger &= u_{\mathbf{k}} c_{\mathbf{k},\sigma}^\dagger + \text{sign}(\sigma) v_{\mathbf{k}} d_{-\mathbf{k},\bar{\sigma}}, \\
\gamma_{\mathbf{k},2,\sigma}^\dagger &= -\text{sign}(\sigma) v_{\mathbf{k}} c_{\mathbf{k},\sigma}^\dagger + u_{\mathbf{k}} d_{-\mathbf{k},\bar{\sigma}},
\end{aligned}
\tag{8}
$$

and we obtain the two quasiparticle bands

$$
\begin{aligned}
E_{\pm,\mathbf{k}} &= \frac{1}{2}(\epsilon_{\mathbf{k}} + \epsilon_d \pm W_{\mathbf{k}}) - \mu, \\
W_{\mathbf{k}} &= \sqrt{(\epsilon_{\mathbf{k}} - \epsilon_d)^2 + \Delta_{cd}^2}, \\
u_{\mathbf{k}} &= \left(\frac{1}{2} - \frac{\epsilon_{\mathbf{k}} - \epsilon_d}{2W_{\mathbf{k}}} \right)^{1/2}, \\
v_{\mathbf{k}} &= \left(\frac{1}{2} + \frac{\epsilon_{\mathbf{k}} - \epsilon_d}{2W_{\mathbf{k}}} \right)^{1/2}.
\end{aligned}
\tag{9}
$$

In the equation for $v_{\mathbf{k}}$, it is assumed that $\Delta_{cd} > 0$. The self-consistency equation for Δ_{cd} becomes

$$1 = \frac{W}{N} \sum_{\mathbf{k}} \frac{1}{W_{\mathbf{k}}} \frac{\sinh\left(\frac{\beta W_{\mathbf{k}}}{2}\right)}{\cosh\left(\frac{\beta W_{\mathbf{k}}}{2}\right) + \cosh\left[\beta\left(\frac{\epsilon_{\mathbf{k}} + \epsilon_d}{2} - \mu\right)\right]}. \quad (10)$$

Next, it is straightforward to show that

$$2N - N_d + N_c = \sum_{\mathbf{k},\sigma} \sum_{\nu=1}^{2} \gamma^{\dagger}_{\mathbf{k},\nu,\sigma} \gamma_{\mathbf{k},\nu,\sigma}, \quad (11)$$

where N_d (N_c) are the operators for the number of c-like (d-like) holes. If we demand that $N_d = N$, the operator N_h of the total hole number becomes

$$N_h = \sum_{\mathbf{k},\sigma} \sum_{\nu=1}^{2} \gamma^{\dagger}_{\mathbf{k},\nu,\sigma} \gamma_{\mathbf{k},\nu,\sigma} \quad (12)$$

so that we have a large Fermi surface, which comprises the localized d holes. This, however, will hold only if there is exactly one localized spin per d site. When Δ_{cd} is zero, the c holes and d holes are decoupled and the condition $N_d = N$ puts a dispersionless d band right at μ, i.e., $\epsilon_d = \mu$. The Fermi surface then is that of the decoupled c holes and accordingly has a volume that does not comprise the d holes.

As already stated for $\Delta_{cd} \to 0$, we have $\epsilon_d \to \mu$ and inserting this into (10) we obtain the equation for the critical temperature

$$1 = \frac{W}{2N} \sum_{\mathbf{k}} \frac{1}{\epsilon_{\mathbf{k}} - \mu} \tanh\left(\frac{\beta_c(\epsilon_{\mathbf{k}} - \mu)}{2}\right). \quad (13)$$

Figure 1 shows T_c as a function of δ.

This is shown both for the true two-dimensional nearest-neighbor-hopping dispersion and for a conduction band with a constant density of states in the interval $[-4t : 4t]$. It is obvious that $T_c \to 0$ as $\delta \to 0$. In the limit of small T_c, we can obtain a rough approximation by replacing the integrand in (13) by $(|\epsilon_{\mathbf{k}} - \mu| + T_c/2)^{-1}$. For the constant density of states, we find in this way

$$T_c = 2t \, e^{-8t/W} \sqrt{\delta(2 - \delta)}. \quad (14)$$

As expected, the energy gain due to the formation of common large Fermi surface thus goes to zero when the density of mobile carriers vanishes. For sufficiently low temperature, the large Fermi surface thus is formed for any carrier concentration, but if there is a competing term in the Hamiltonian, there may be a phase transition at finite doping.

We now introduce the d-d Heisenberg exchange $\propto J$. We decouple the d-d Heisenberg exchange in the same way as the c-d exchange:

$$\vec{S}_{d,i} \cdot \vec{S}_{d,j} - \frac{n_{d,i} n_{d,j}}{4} = -\frac{1}{2} s^{\dagger}_{ij} s_{ij},$$

$$s^{\dagger}_{ij} = d^{\dagger}_{i,\uparrow} d^{\dagger}_{j,\downarrow} - d^{\dagger}_{i,\downarrow} d^{\dagger}_{j,\uparrow},$$

$$s^{\dagger}_{ij} s_{ij} \approx \langle s^{\dagger}_{ij} \rangle s_{ij} + s^{\dagger}_{ij} \langle s_{ij} \rangle - \langle s^{\dagger}_{ij} \rangle \langle s_{ij} \rangle.$$
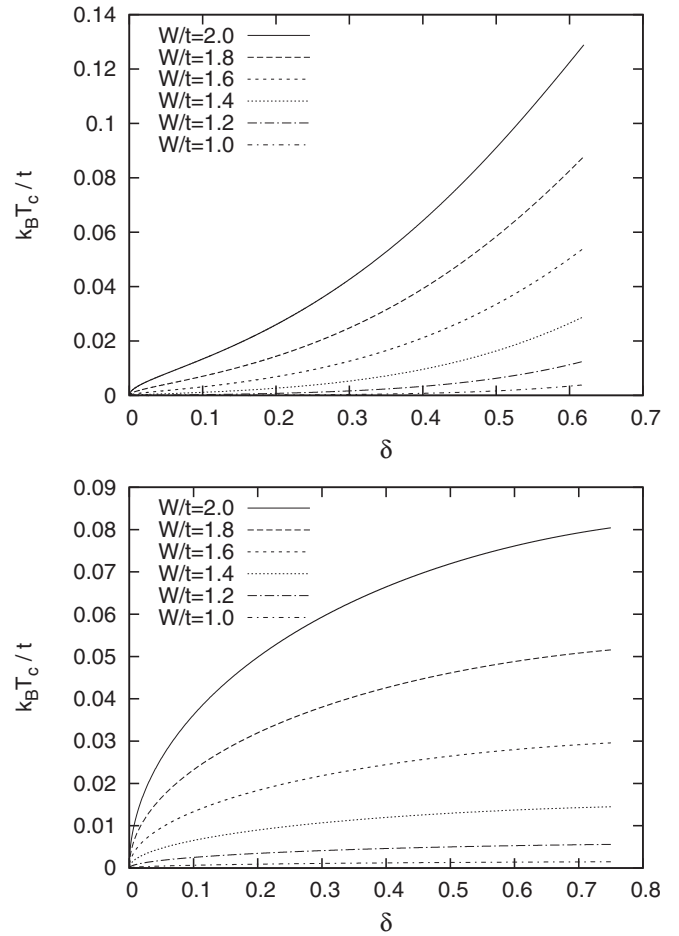
FIG. 1. Critical temperature for the onset of the parameter Δ_{cd} with the true two-dimensional nearest-neighbor-hopping band structure (top) and a constant density of states in the interval $[-4t : 4t]$ (bottom).

Inclusion of this term doubles the dimension of the matrices to be considered. Introducing $v_{\mathbf{k}} = (c^{\dagger}_{\mathbf{k},\uparrow}, d_{-\mathbf{k},\downarrow}, c_{-\mathbf{k},\downarrow}, d^{\dagger}_{\mathbf{k},\uparrow})$, the Hamiltonian matrix becomes

$$H = \sum_{\mathbf{k}} v^{\dagger}_{\mathbf{k}} H_{\mathbf{k}} v_{\mathbf{k}},$$

$$H_{\mathbf{k}} = \begin{pmatrix} \epsilon_{\mathbf{k}} - \mu & -\frac{\Delta_{cd}}{2} & 0 & 0 \\ -\frac{\Delta_{cd}}{2} & \epsilon_d - \mu & 0 & -\Delta_{dd}\gamma_{\mathbf{k}} \\ 0 & 0 & -\epsilon_{\mathbf{k}} + \mu & -\frac{\Delta_{cd}}{2} \\ 0 & -\Delta_{dd}\gamma_{\mathbf{k}} & -\frac{\Delta_{cd}}{2} & -\epsilon_d + \mu \end{pmatrix},$$

$$\gamma_{\mathbf{k}} = \frac{1}{2}[\cos(k_x) \pm \cos(k_y)],$$

$$\Delta_{dd} = \frac{zJ}{2} \langle s_{ij} \rangle. \quad (15)$$

The two parameters Δ_{cd} and Δ_{dd} now have to be determined self-consistently. Unlike the on-site order parameter Δ_{cd}, the d-d pairing amplitude is a bond-related quantity and, thus, may have different sign for bonds along x and y so that we may have s-like pairing or d-like pairing. These two possibilities have to be considered separately.

Before studying the full problem, we briefly consider the case $\Delta_{cd} = 0$. In this case, the d and c holes are again

decoupled and we only have to treat the d-electron system. The chemical potential μ is determined by the conduction holes alone and we must have $\epsilon_d = \mu$. The result will not depend on δ or W and the temperature dependence is universal if temperature is measured in units of J. Finally, there is no difference between $\gamma_{s,d}(\mathbf{k})$ because $\cos(k_y) = -\cos(k_y + \pi)$ so that the d-like pairing simply corresponds to a shift of the Brillouin zone by $(\pi,0)$. The self-consistency equation reads as

$$\Delta_{dd} = \frac{2J}{N} \sum_{\mathbf{k}} \gamma(\mathbf{k}) \frac{\sinh[\beta\gamma(\mathbf{k})\Delta_{dd}]}{1 + \cosh[\beta\gamma(\mathbf{k})\Delta_{dd}]} \qquad (16)$$

and the temperature for the phase transition is $\tilde{T}_c = J/4$. The gap at $T = 0$ is found to be

$$\Delta_{dd} = \frac{2J}{N} \sum_{\mathbf{k}} |\gamma(\mathbf{k})| = J \cdot 0.81. \qquad (17)$$

The localized spins acquire a nonvanishing dispersion, which is unphysical and an artifact of the mean-field approximation. The problem is somewhat lessened in that the localized electrons at least have no Fermi surface. To see this, we note first that the dispersion consists of two bands $\epsilon_d \pm \Delta_{dd}\gamma(\mathbf{k})$. Since $\epsilon_d = \mu$, the lower of these is completely filled. The momentum distribution function for the d electrons then becomes

$$n_{d,\mathbf{k}} = \sum_{\sigma} \langle d^{\dagger}_{\mathbf{k},\sigma} d_{\mathbf{k},\sigma} \rangle = 1 \qquad (18)$$

so that at least the momentum distribution of the d electrons is consistent with localized electrons.

Next we switch to the full problem of two coupled order parameters, i.e., $\Delta_{cd} \neq 0$ and $\Delta_{dd} \neq 0$. All results presented below have been obtained by numerical solution of the self-consistency equations on a 400×400 lattice with periodic boundary conditions. Study of the variation with lattice size shows that this implies a reasonable convergence.

As already mentioned, Δ_{dd} may be s like and $d_{x^2-y^2}$ like. This difference will now matter because the relative position of the lines of zeros in the d-electron dispersion and the Fermi surface of the c electrons makes a physical difference. To decide which of the two symmetries is realized, we consider the free energy per site given by

$$f(T,n) = -\frac{1}{\beta N} \sum_{\mathbf{k}} \sum_{\nu=1}^{4} \log(1 + e^{-\beta E_{\mathbf{k},\nu}})$$
$$+ \frac{\Delta_{cd}^2}{2W} + \frac{\Delta_{dd}^2}{4J} + (\delta - 1)\mu. \qquad (19)$$

Numerical evaluation shows that the s-like state is never realized. Figure 2 then shows an example of the development of the two coupled order parameters as J is switched on.

It is quite obvious that increasing Δ_{dd} is detrimental to Δ_{cd}, i.e., the two order parameters are competing. Nonvanishing J thus may introduce a phase transition at $T = 0$ as a function of doping between the two phases. To discuss the phase diagram, we note first that we can distinguish two regimes: at low doping the critical temperature T_c for the onset of Δ_{cd} will be below $J/4$, which is the critical temperature for the onset of Δ_{dd}. This means that, as the temperature is lowered, a nonvanishing Δ_{dd} sets in first and Δ_{cd} then must develop on the background of this nonvanishing Δ_{dd}. When $T_c > J/4$, on the other hand,
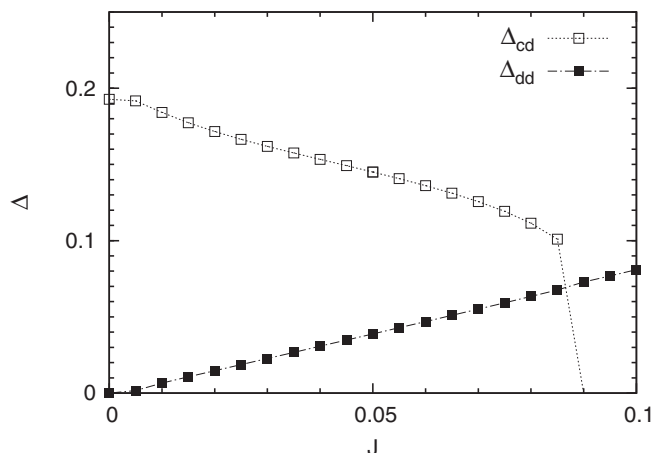
FIG. 2. Development of the two order parameters with increasing J. The other values are $W/t = 1.6$, $\delta = 0.2$, and $T/t = 0.001$.

we first have a nonvanishing Δ_{cd} and Δ_{dd} develops at lower temperature. As will be seen next, the two regimes are more different than might be expected at first sight. For the time being, we fix $W/t = 1.6$ and $J/t = 0.05$. As can be seen in Fig. 1, the doping where $T_c = J/4$ then is approximately $\delta = 0.3$.

Figure 3 then shows the self-consistent Δ's as a function of temperature for $\delta = 0.32$. Both parameters show a fairly conventional behavior at the two phase transitions with the characteristic $\sqrt{T_c - T}$ behavior and the same is seen whenever Δ_{cd} sets in at higher temperature.

The situation is quite different for $\delta < 0.3$, as can be seen in Fig. 4. For most dopings, there is now a small but finite temperature range where two solutions ($\Delta_{cd} \neq 0$, $\Delta_{dd} \neq 0$) exist (in addition there are the solutions with $\Delta_{dd} = 0$ and $\Delta_{cd} = 0$). Calculation of the free energy shows that it is always the solution with the higher Δ_{cd} that has the lower free energy, i.e., this is the physical state.

To clarify the nature of the phase transition, we fix Δ_{cd}, determine all other parameters ($\mu, \epsilon_d, \Delta_{dd}$) self-consistently, and evaluate the free energy f as a function of Δ_{cd}. Points on the resulting curve $f(\Delta_{cd})$, which are stationary with
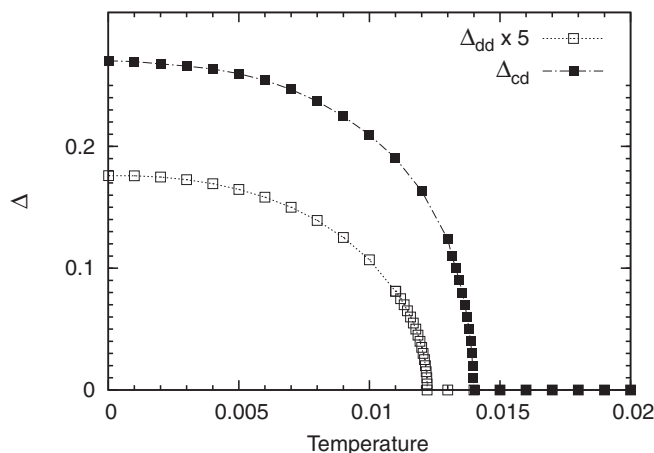
FIG. 3. Temperature dependence of the two order parameters for $W/t = 1.6$, $J/t = 0.05$, and $\delta = 0.32$.
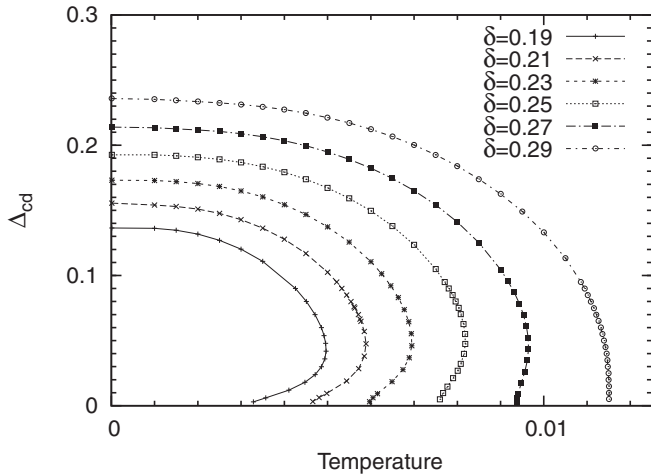
FIG. 4. Self-consistent solution for Δ_{cd} as a function of temperature for various dopings δ. The other values are $W/t = 1.6$ and $J/t = 0.05$.

respect to variations of Δ_{cd}, are stationary with respect to variations of all parameters and therefore are solutions to the self-consistency equations. The result is shown in Fig. 5. At high temperature, $f(\Delta_{cd})$ has only one extremum, namely, a minimum at $\Delta_{cd} = 0$. As the temperature is lowered, however,
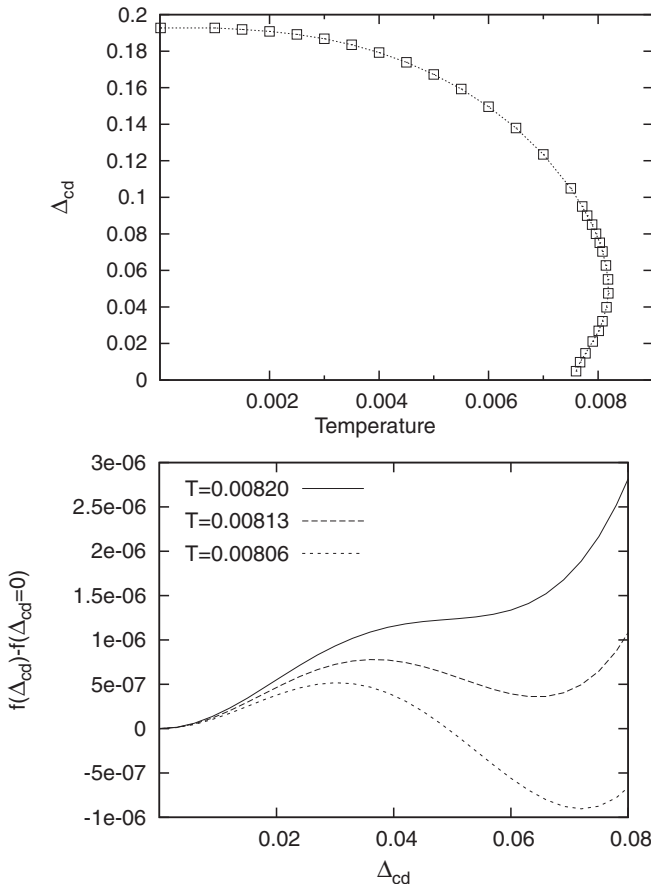
FIG. 5. Top panel: Self-consistent solution for Δ_{cd} as a function of temperature for $\delta = 0.25$ (see Fig. 4). Bottom panel: Scans of the free energy as a function of Δ_{cd} whereby all other mean-field parameters have been obtained self-consistently.
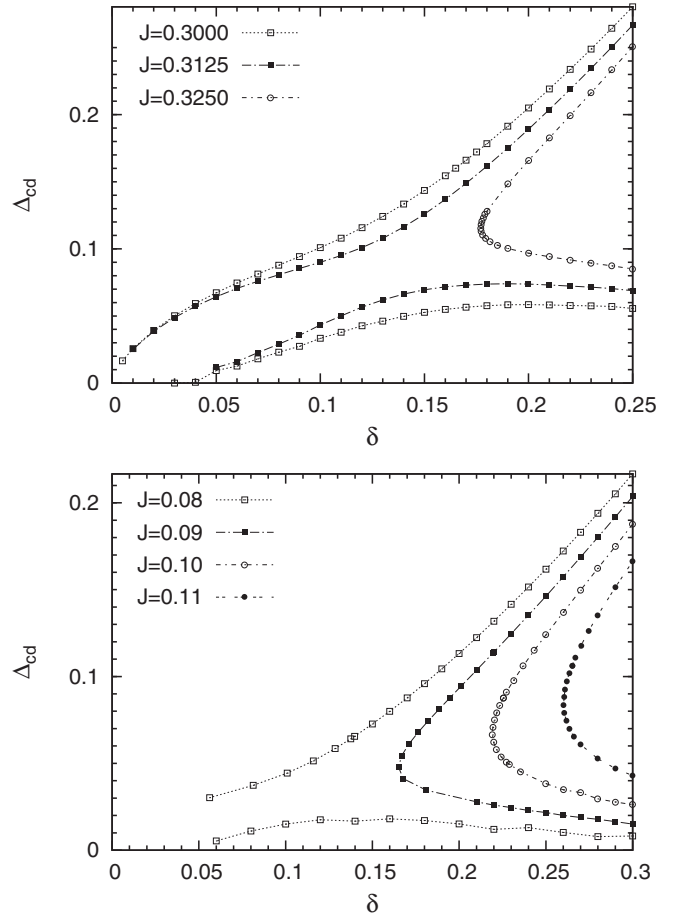
FIG. 6. Self-consistent solutions for Δ_{cd} as a function of doping for $T = 0$ and different J. The value $W/t = 2$ ($W/t = 1.6$) in the upper (lower) panel of the figure.

one can recognize a "wiggle" in the curve, which develops into a maximum and a minimum. These correspond to the two solutions with nonvanishing Δ_{cd}. Next, there occurs a level crossing between the two minima (we thus have a first order transition), and as the temperature is lowered further, the maximum for $\Delta_{cd} \neq 0$ "absorbs" the minimum at $\Delta_{cd} = 0$. From then on, we have only the minimum with $\Delta_{cd} \neq 0$ and the maximum at $\Delta_{cd} = 0$. This behavior can be seen at almost all dopings below $\tilde{\delta}$. It is only very close to $\tilde{\delta}$ that there is only one solution, but the $\Delta_{cd}(T)$ curve is very steep as $\Delta_{cd} \to 0$. The important finding then is that the temperature-induced transition between small and large Fermi surface is a first-order transition in this doping range. This is not surprising in that a second-order transition involving competing order parameters may become first order.[53]

Next we consider the dependence on hole doping δ, in particular, the question if the Fermi surface transition now occurs at finite doping even at zero temperature. Figure 6, which shows the self-consistent solutions for Δ_{cd} at $T = 0$ for different W/t and J/t, demonstrates that the answer depends on the magnitude of J/t. For small J, a nonvanishing solution exists down to $\delta = 0$. In fact, there are two such solutions, but computation of the free energy shows that only the solution with the larger Δ_{cd} is a minimum and moreover has a lower free energy than the solution with $\Delta_{cd} = 0$. Accordingly, there is no
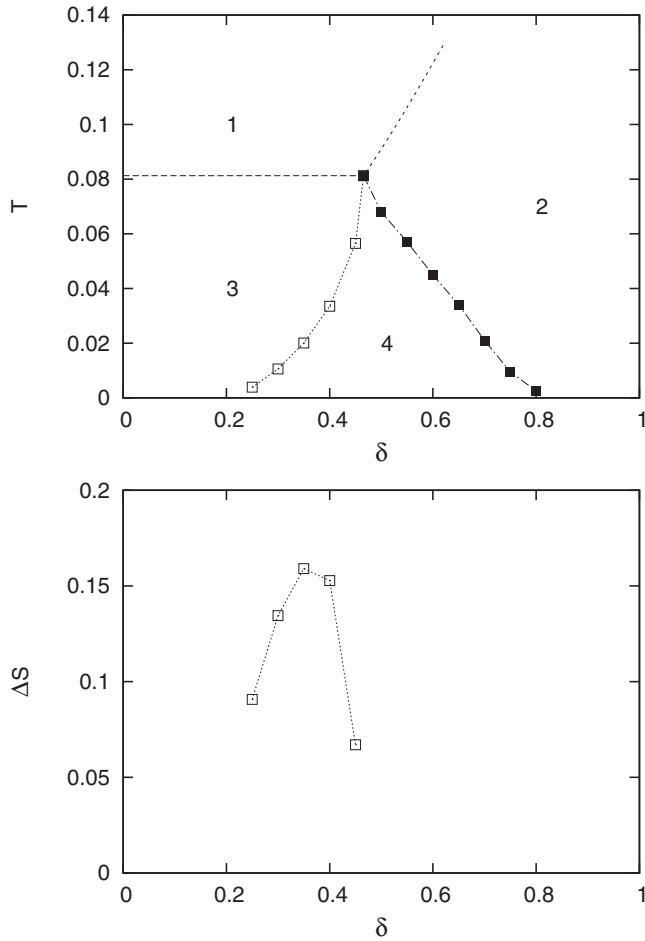
FIG. 7. Top panel: Mean-field phase diagram for the parameter values $W/t = 2$ and $J/t = 0.325$. Bottom panel: Difference in entropy per site between the phases 3 and 4.

FIG. 8. Top panel: Band structure for phase 2 ($T = 0.005$, $\delta = 0.60$). The two vertical lines at μ give the Fermi momenta, i.e., the crossings of the quasiparticle band through μ. Bottom panel: Band structure for phase 3 ($T = 0.005$, $\Delta = 0.25$). Other parameter values are $W/t = 2$ and $J/t = 0.325$.

phase transition down to $\delta = 0$ for small J/t. If J increases, however, there is now an extended range of small δ where no solution with $\Delta_{cd} \neq 0$ exists. As can be seen in Fig. 6, this change occurs in that the maximum and minimum of $f(\Delta_{cd})$ "merge" for some δ. The hourglass shape formed by the two $\Delta_{cd}(\delta)$ curves immediately below the critical J/t can be clearly seen in the upper part of the figure. It has been verified, however, that, for large values of J/t where the transition has occurred, there is no more solution for low δ. This means that, for larger J/t, a phase transition does occur and there is a considerable range of δ where the mean-field theory predicts a spin liquid (i.e., $\Delta_{dd} \neq 0$) with a small Fermi surface.

We proceed to a discussion of the phase diagram whereby we consider the more interesting case of larger J/t. An example is shown in Fig. 7, and the band structures for the various phases are shown in Figs. 8 and 9.

To begin with, we can distinguish four phases. At high temperature (phase 1), both self-consistent parameters are zero, which implies that the conduction holes are decoupled from the localized spins and the localized spins themselves are uncorrelated. At higher doping and low temperature, there is a phase with $\Delta_{cd} \neq 0$, $\Delta_{dd} = 0$ (phase 2). The band structure (see Fig. 8, top panel) shows that there is a large Fermi surface with an enhanced band mass. This

phase most likely corresponds to the overdoped regime in cuprate superconductors. For low doping and low temperature, on the other hand, there is a phase with $\Delta_{dd} \neq 0$, $\Delta_{cd} = 0$ (phase 3). This has strong singlet correlations between the localized spins and a small Fermi surface, which is centered at (π, π) in mean-field theory (see Fig. 8, bottom panel). This phase likely corresponds to the "pseudogap" phase in cuprate superconductors. Thereby, the strongest deficiency of the mean-field theory consists in the neglect of any correlation between the localized spins and the conduction holes. One may expect that coupling of the conduction hole pocket around (π, π) to the antiferromagnetic spin fluctuations of the localized spins will create hole pockets centered near $(\frac{\pi}{2}, \frac{\pi}{2})$. In any way, however, the Fermi surface does not comprise the d electrons in this phase. Finally, at intermediate doping and low temperature, there is a domelike region in the phase diagram in which both self-consistent parameters are different from zero (phase 4). Inspection of the band structure in Fig. 9 shows that phase 4 does not have a Fermi surface, but rather a gap with a node along the $(1,1)$ direction, i.e., the band structure expected for a superconductor with $d_{x^2-y^2}$ order parameter. The Fermi momentum along the $(1,1)$ direction coincides with that of the large Fermi surface, however, so that we have a gapped large Fermi surface in this phase. Across the phase transition on the low-doping part of the dome, the Fermi surface thus changes from a hole pocket centered on (π, π) to a gapped large Fermi surface, whereas the transition on the high-doping side of the dome corresponds to the opening of a $d_{x^2-y^2}$-like gap on the large Fermi surface. Accordingly, we consider the question as to whether phase 4 is superconducting. To that end, we consider the c-like pairing amplitude

$$\Delta_{cc} = \frac{1}{N} \sum_{\mathbf{k}} \gamma(\mathbf{k}) \langle c^\dagger_{\mathbf{k}\uparrow} c^\dagger_{-\mathbf{k}\downarrow} + c_{-\mathbf{k}\downarrow} c_{\mathbf{k}\uparrow} \rangle. \qquad (20)$$
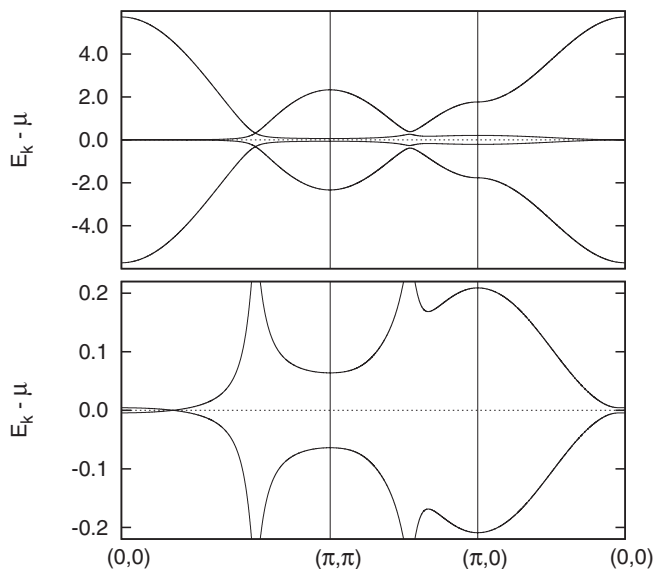
FIG. 9. Band structure for phase 4 ($T = 0.005$, $\delta = 0.45$). Entire bandwidth (top panel) and closeup of the region near μ (bottom panel). Other parameter values are $W/t = 2$ and $J/t = 0.325$.

Figure 10 shows that this is indeed different from zero within the phase 4. Interestingly, the Hamiltonian does not contain any attractive interaction between the conduction holes. Rather, the singlet pairing between the localized spins as described by the parameter Δ_{dd} is transferred to the mobile conduction hole system by the coherent Kondo pairing amplitude Δ_{cd}.

Figure 11 shows the gap and the c-like spectral weight for several momenta along the (1,0) direction and demonstrates that the present theory qualitatively reproduces a well-known anomaly in cuprate superconductors: Whereas the gap size near (π,0) increases with decreasing T_c (in contrast to what one expects from BCS theory), the spectral weight decreases to zero.[54,55] At least the behavior in Fig. 11 is easy to understand: The gap size around (π,0) is determined by Δ_{dd} and the c-like spectral weight by Δ_{cd}, which governs the degree of mixing between c- and d-like bands. Lower T_c implies a lower value
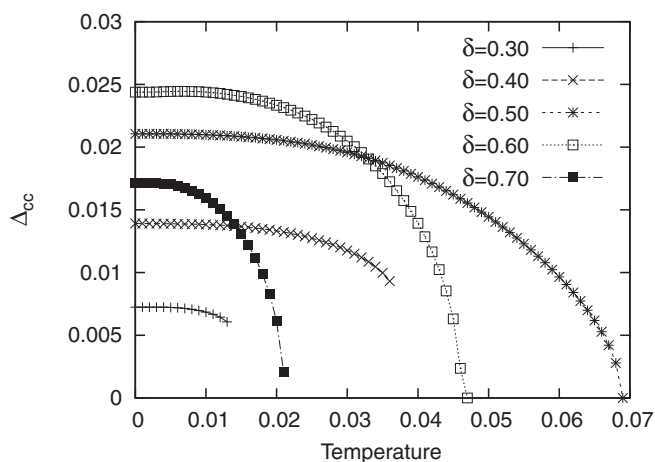
FIG. 10. Pairing amplitude for conduction holes Δ_{cc} as a function of temperature. Other parameter values are $W/t = 2.0$ and $J/t = 0.325$.
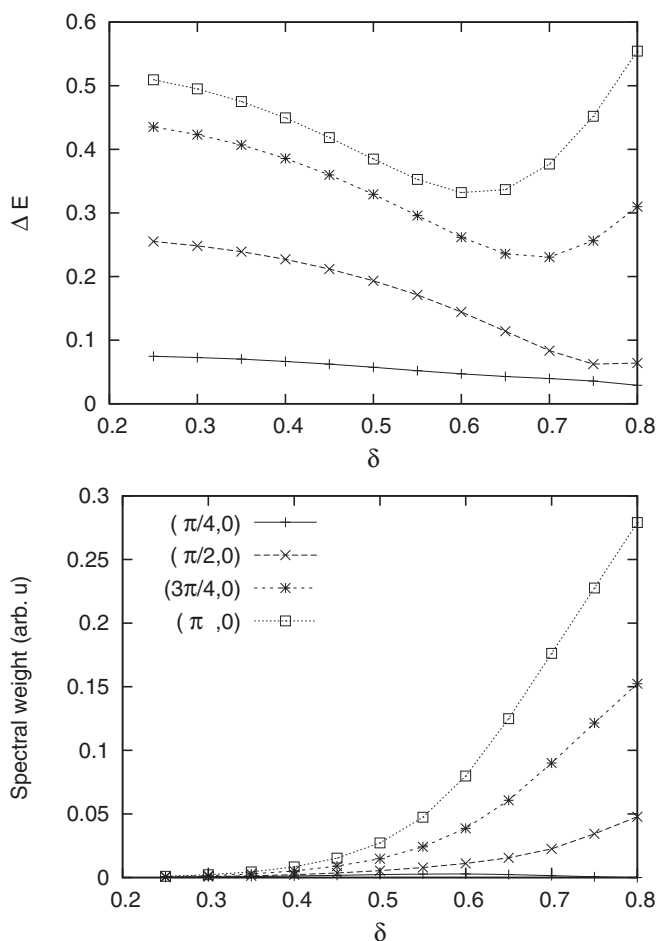
FIG. 11. Energy gap (top panel) and spectral weight of the band below μ (bottom panel) as a function of doping for some momenta along (1,0). Parameter values are $W/t = 2.0$, $J/t = 0.325$, and $T/t = 0.05$.

of Δ_{cd} at low T and, since the two parameters compete with each other, a larger value of Δ_{dd}.

To conclude this section, we briefly summarize the results of the the mean-field theory. The competition between Kondo coupling and Heisenberg exchange between localized spins leads to a doping driven phase transition between states with different Fermi surface volume. The phase for high doping is characterized by a complex order parameter that describes coherent singlet pairing between localized and conduction holes and leads to a Fermi surface volume that includes the localized spins. The low-doping phase is characterized by an order parameter that describes singlet correlations between the localized spins, and there is no coupling between conduction holes and localized spins. The Fermi surface, thus, is a hole pocket with a volume that does not include the localized spins. Interestingly, there is an intermediate phase where both order parameters coexist. This phase has a gapped large Fermi surface and shows superconducting correlations between the conduction holes. These may be interpreted as the singlet correlations between the localized spins being transferred to the conduction electrons by the coherent Kondo singlet formation. This implies that the superconducting transition has a very different character on the underdoped and overdoped side of the superconducting dome. Whereas on the overdoped

side the transition looks fairly conventional, with a gap opening in the large Fermi surface, on the underdoped side, the transition corresponds to the sudden emergence of a gapped large Fermi surface from the high-temperature phase with a hole pocket. A somewhat discomforting feature of the transition in the underdoped range is the fact that it is first order. Lastly, we mention that the criticial temperatures and dopings in this study are very different from the cuprates, but this can be hardly a surprise because we are studying a different model (single-band Kondo lattice rather than Kondo-Heisenberg model) and mean-field theories can not be expected to produce quantitatively correct transition temperatures anyway.

III. STRONG-COUPLING THEORY: SMALL FERMI SURFACE

The mean-field theory in the preceding section may be expected to be good for $t \gg W, J$ although, even there, relaxing the constraint on the occupation of the d orbital is problematic. The physical regime of parameters, however, is rather $W \gg t \gg J$. In fact, a considerable deficiency of the mean-field treatment lies in the fact that, in the hole pocket phase, the d and c holes are completely decoupled from one another, which clearly is unrealistic for large W/t. In the following sections, we therefore give a description of the two phases in a strong-coupling picture, which may be expected to hold best in the limit $W/t \gg 1$. The discussion of the small Fermi surface phase in this section thereby closely follows the theory for the lightly doped Mott insulator given in Ref. 49.

The essence of the strong-coupling theory is the approximate diagonalization of the Hamiltonian in a suitably chosen truncated Hilbert space. To construct this truncated Hilbert space for the small Fermi surface state, we start from the case $\delta = 0$ and consider a state $|\Psi_0\rangle$ of the d-spin system, which has exactly one electron per site, is invariant under point-group operations, has momentum zero, and is a spin singlet. These are the quantum numbers of a vacuum state and indeed $|\Psi_0\rangle$ will play the role of the vacuum state in our analysis. The only property of $|\Psi_0\rangle$ that is relevant for the quasiparticle dispersion and total energy is the static spin-correlation function

$$\chi_{ij} = \langle \Psi_0 | \mathbf{S}_i \cdot \mathbf{S}_j | \Psi_0 \rangle. \tag{21}$$

We consider χ_{ij} as a given input parameter. We assume it to be antiferromagnetic and of short range, i.e.,

$$\chi_{ij} = C_0 \, e^{i\mathbf{Q}\cdot(\mathbf{R}_i - \mathbf{R}_j)} e^{-\frac{|\mathbf{R}_i - \mathbf{R}_j|}{\zeta}}, \tag{22}$$

where $\mathbf{Q} = (\pi, \pi)$. A more detailed discussion is given in Ref. 49. It will be seen below that within the framework of the present theory, only the nearest-neighbor spin correlation χ_{10} has any relevance for the results.

Next, we define the following operators, which add a conduction hole to the system:

$$\hat{a}_{i,\uparrow}^\dagger = \frac{1}{\sqrt{2}} (\hat{c}_{i,\uparrow}^\dagger \hat{N}_{i\downarrow} - \hat{c}_{i,\downarrow}^\dagger S_i^+),$$

$$\hat{b}_{i,1,\uparrow}^\dagger = \frac{1}{\sqrt{2}} (\hat{c}_{i,\uparrow}^\dagger \hat{N}_{i\downarrow} + \hat{c}_{i,\downarrow}^\dagger S_i^+), \tag{23}$$

$$\hat{b}_{i,2,\uparrow}^\dagger = \hat{c}_{i,\uparrow}^\dagger \hat{N}_{i\uparrow}.$$

Here capital (small) letters are used for localized (conduction) holes $\hat{c}_{i,\sigma} = c_{i,\sigma}(1 - n_{\bar{\sigma}})$ and $\hat{N}_{i,\sigma} = N_{i,\sigma}(1 - N_{\bar{\sigma}})$. The operators in Eq. (23) add a conduction hole to the system, thereby changing the z component of the total spin by $+1/2$ and producing either a local singlet ($\hat{a}_{i,\uparrow}^\dagger$) or one of the two components of a local triplet ($\hat{b}_{i,1,\uparrow}^\dagger$ and $\hat{b}_{i,2,\uparrow}^\dagger$). Analogous operators that change the z component of the total spin by $-\frac{1}{2}$ are easily constructed. By using these operators, we can now write down the basis states of the truncated Hilbert space as

$$2^{(N_\nu + N_\mu + N_\lambda)/2} \left(\prod_{\nu=1}^{N_\nu} \hat{a}_{i_\nu, \sigma_\nu}^\dagger \right) \left(\prod_{\mu=1}^{N_\mu} \hat{b}_{i_\mu, 1, \sigma_\mu}^\dagger \right) \left(\prod_{\lambda=1}^{N_\lambda} \hat{b}_{i_\lambda, 2, \sigma_\lambda}^\dagger \right) |\Psi_0\rangle. \tag{24}$$

It is thereby understood that all sites $(i_\nu, j_\mu, k_\lambda)$ are pairwise different from each other, which means that no two operators are allowed to act on the same site. The states (24) have singlets and triplets at specified positions and we will treat these as spin-$\frac{1}{2}$ fermions with a hard-core constraint, which is the key approximation of the theory. Fermions are the only meaningful description for these particles because operators of the type (23), which refer to different sites, anticommute. Since $\langle \Psi_0 | \hat{a}_{i,\uparrow} \hat{a}_{i,\uparrow}^\dagger | \Psi_0 \rangle = \langle \Psi_0 | \hat{b}_{i,1,\uparrow} \hat{b}_{i,1,\uparrow}^\dagger | \Psi_0 \rangle = \langle \Psi_0 | \hat{b}_{i,2,\uparrow} \hat{b}_{i,2,\uparrow}^\dagger | \Psi_0 \rangle = \frac{1}{2}$, the states (24) are approximately normalized. The issue of the normalization of the states has been discussed in detail in Ref. 49, where it was concluded that this normalization will be a good approximation in the limit of short spin-correlation length ζ, which means the case of a spin liquid, which is the case of interest, e.g., in the underdoped cuprates. A more detailed discussion of this issue and others is given in the Appendix.

As already stated, we treat the singlets and triplets as fermionic quasiparticles, i.e., the states (24) are represented by states of Fermionic spin-$\frac{1}{2}$ quasiparticles

$$\left(\prod_{\nu=1}^{\hat{N}_\nu} a_{i_\nu, \sigma_\nu}^\dagger \right) \left(\prod_{\mu=1}^{\hat{N}_\mu} b_{i_\mu, 1, \sigma_\mu}^\dagger \right) \left(\prod_{\lambda=1}^{\hat{N}_\lambda} b_{i_\lambda, 2, \sigma_\lambda}^\dagger \right) |\Psi_0\rangle. \tag{25}$$

Operators in the quasiparticle Hilbert space then are defined by demanding that their matrix elements between the states (25) are identical to those of the physical operators between the corresponding states (24).

We illustrate this by setting up the quasiparticle Hamiltonian. Straightforward calculation gives the following matrix elements in the physical Hilbert space:

$$\langle \Psi_0 | \hat{a}_{j,\uparrow} H_t \hat{a}_{i,\uparrow}^\dagger | \Psi_0 \rangle = -t_{ij} \left(\frac{1}{8} + \frac{\chi_{ij}}{2} \right),$$

$$\langle \Psi_0 | \hat{b}_{j,1,\uparrow} H_t \hat{a}_{i,\uparrow}^\dagger | \Psi_0 \rangle = -t_{ij} \left(\frac{1}{8} - \frac{\chi_{ij}}{6} \right),$$

$$\langle \Psi_0 | \hat{b}_{j,2,\uparrow} H_t \hat{a}_{i\uparrow}^\dagger | \Psi_0 \rangle = -t_{ij} \left(\frac{1}{4\sqrt{2}} - \frac{\chi_{ij}}{3\sqrt{2}} \right),$$

$$\langle \Psi_0 | \hat{b}_{j,1,\uparrow} H_t \hat{b}_{i,1,\uparrow}^\dagger | \Psi_0 \rangle = -t_{ij} \left(\frac{1}{8} + \frac{\chi_{ij}}{2} \right),$$

$$\langle\Psi_0|\hat{b}_{j,2,\uparrow}H_t\hat{b}_{i,1,1\uparrow}^\dagger|\Psi_0\rangle = -t_{ij}\left(\frac{1}{4\sqrt{2}}+\frac{\chi_{ij}}{3\sqrt{2}}\right),$$

$$\langle\Psi_0|\hat{b}_{j,2,\uparrow}H_t\hat{b}_{i,2,\uparrow}^\dagger|\Psi_0\rangle = -t_{ij}\left(\frac{1}{4}+\frac{\chi_{ij}}{3}\right). \quad (26)$$

They represent the decomposition of hopping into events of annihilation and creation of singlets and triplets. The hopping term H_t for the quasiparticles thus takes the form

$$H_t = \sum_{i,j}\sum_\sigma \mathbf{v}_{i,\sigma}^\dagger \mathbf{T}_{ij}\mathbf{v}_{j,\sigma}, \quad (27)$$

where

$$\mathbf{v}_{i,\sigma}^\dagger = (a_{i,\sigma}^\dagger, b_{i,1,\sigma}^\dagger, b_{i,2,\sigma}^\dagger) \quad (28)$$

and

$$\mathbf{T}_{ij} = t_{ij}\begin{pmatrix} \frac{1}{4}+\chi_{ij} & \frac{1}{4}-\frac{\chi_{ij}}{3} & \sqrt{2}\left(\frac{1}{4}-\frac{\chi_{ij}}{3}\right) \\ \frac{1}{4}-\frac{\chi_{ij}}{3} & \frac{1}{4}+\chi_{ij} & \sqrt{2}\left(\frac{1}{4}+\frac{\chi_{ij}}{3}\right) \\ \sqrt{2}\left(\frac{1}{4}-\frac{\chi_{ij}}{3}\right) & \sqrt{2}\left(\frac{1}{4}+\frac{\chi_{ij}}{3}\right) & \frac{1}{2}+\frac{2\chi_{ij}}{3} \end{pmatrix}. \quad (29)$$

We thereby have to keep in mind the hard-core constraint between the quasiparticles. In addition, it has been assumed that nearby quasiparticles do not modify the matrix elements describing the propagation of a given quasiparticle substantially. Again, this will be justified in the limit of short spin-correlation length ζ. The key simplification is that, in our restricted Hilbert space, the Kondo-coupling term H_W takes the simple form

$$H_W = -\frac{3W}{4}\sum_{i,\sigma}a_{i\sigma}^\dagger a_{i\sigma} + \frac{W}{4}\sum_{i,\sigma}\sum_{n=1}^{2}b_{i,n,\sigma}^\dagger b_{i,n,\sigma}. \quad (30)$$

In the strong-coupling limit $W/t \gg 1$, we thus expect to obtain something like one lower and two upper Hubbard bands separated by an energy of order W.

It remains to represent H_J in the new basis. Straightforward computation gives the following matrix elements in the physical Hilbert space:

$$\langle\Psi_0|\hat{a}_{i,\uparrow}(\mathbf{S}_i\cdot\mathbf{S}_j)\hat{a}_{i,\uparrow}^\dagger|\Psi_0\rangle = 0,$$

$$\langle\Psi_0|\hat{b}_{i,1,\uparrow}(\mathbf{S}_i\cdot\mathbf{S}_j)\hat{a}_{i,\uparrow}^\dagger|\Psi_0\rangle = \frac{\chi_{ij}}{6},$$

$$\langle\Psi_0|\hat{b}_{i,2,\uparrow}(\mathbf{S}_i\cdot\mathbf{S}_j)\hat{a}_{i,\uparrow}^\dagger|\Psi_0\rangle = \frac{\chi_{ij}}{3\sqrt{2}},$$

$$\langle\Psi_0|\hat{b}_{i,1,\uparrow}(\mathbf{S}_i\cdot\mathbf{S}_j)\hat{b}_{j,1,\uparrow}^\dagger|\Psi_0\rangle = 0, \quad (31)$$

$$\langle\Psi_0|\hat{b}_{i,2,\uparrow}(\mathbf{S}_i\cdot\mathbf{S}_j)\hat{b}_{i,1,\uparrow}^\dagger|\Psi_0\rangle = \frac{\chi_{ij}}{3\sqrt{2}},$$

$$\langle\Psi_0|\hat{b}_{i,2,\uparrow}(\mathbf{S}_i\cdot\mathbf{S}_j)\hat{b}_{i,2,\uparrow}^\dagger|\Psi_0\rangle = \frac{\chi_{ij}}{6}$$

so that the d-d exchange for the quasiparticles takes the form

$$H_J = zJ\chi_{10}\sum_i\sum_\sigma \mathbf{v}_{i,\sigma}^\dagger K\mathbf{v}_{i,\sigma} + \frac{zNJ\chi_{10}}{2}, \quad (32)$$

where χ_{10} denotes the nearest-neighbor spin-correlation function and

$$\mathbf{K} = \begin{pmatrix} -1 & \frac{1}{3} & \frac{\sqrt{2}}{3} \\ \frac{1}{3} & -1 & \frac{\sqrt{2}}{3} \\ \frac{\sqrt{2}}{3} & \frac{\sqrt{2}}{3} & -\frac{2}{3} \end{pmatrix}. \quad (33)$$

The additional constant is the contribution from the spin background whereby the correction due to the z broken bonds per quasiparticle is accounted for in the first term. The exchange term also has matrix elements of the type

$$\langle\Psi_0|\hat{b}_{i,1,\uparrow}\hat{b}_{j,1,\uparrow}(\mathbf{S}_i\cdot\mathbf{S}_j)\hat{a}_{i,\uparrow}^\dagger\hat{a}_{i,\uparrow}^\dagger|\Psi_0\rangle = \frac{1}{16}+\frac{\chi_{ij}}{12}. \quad (34)$$

Their contribution to the total energy will be $\propto\delta^2$ and we will neglect these.

Next we consider the hole count. The number of localized holes always is N, the number of sites in the system, whereas a self-evident expression for the number of conduction holes is

$$N_c = \sum_{\mathbf{k},\sigma}(a_{\mathbf{k},\sigma}^\dagger a_{\mathbf{k},\sigma} + b_{\mathbf{k},1,\sigma}^\dagger b_{\mathbf{k},1,\sigma} + b_{\mathbf{k},2,\sigma}^\dagger b_{\mathbf{k},2,\sigma}). \quad (35)$$

This will give rise to a Fermi surface, the volume of which corresponds to the doped holes but does not include the d-electrons.

The resulting quasiparticle band structure is shown in Fig. 12. For a low density of quasiparticles, it will be a reasonable approximation to neglect the hard-core constraint because the probability that two particles occupy the same site and thus violate the constraint is small.

The Fermi surface then takes the form of a hole pocket centered at $\mathbf{Q} = (\pi,\pi)$. For a semiquantitative discussion, we may use second-order perturbation theory for the dispersion $\epsilon_{1,\mathbf{k}}$ of the lowest quasiparticle band around $\mathbf{Q}$. This gives

$$E_{\mathbf{k}} = -\frac{3W}{4}+\left(\frac{1}{4}+\chi_{10}\right)\epsilon_{\mathbf{k}} - \frac{3}{W}\left(\frac{1}{4}-\frac{\chi_{10}}{3}\right)^2\epsilon_{\mathbf{k}}^2. \quad (36)$$
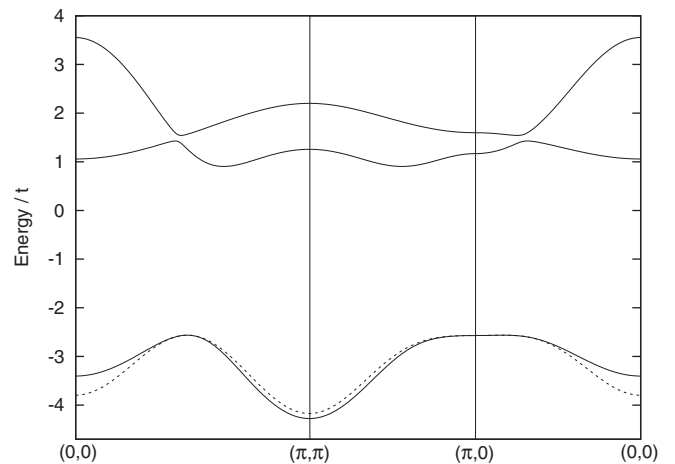
FIG. 12. Dispersion of the quasiparticle bands for the phase with small Fermi surface. Parameter values are $W/t = 4$, $J/t = 4$, and $\chi_{10} = -0.28$. The dashed line is the dispersion of the lowest band as obtained by second-order perturbation theory.

The band minimum is at $(0,0)$ for $\chi_{10} > -\frac{1}{4}$ and at (π,π) otherwise. The third term on the right-hand side favors a χ_{10} that is positive, and the contribution from the spin background favors a negative χ_{10}.

By introducing $\kappa = \mathbf{k} - \mathbf{Q}$ or $\kappa = \mathbf{k}$, depending on whether the minimum of the dispersion is at $\mathbf{k} = (\pi,\pi)$ or $\mathbf{k} = (0,0)$, we find

$$\epsilon_{1,\mathbf{k}} = c_0 + c_1\kappa^2,$$
$$c_0 = -\frac{3W}{4} \mp 4t\left(\frac{1}{4} + \chi_{10}\right) - \frac{48t^2}{W}\left(\frac{1}{4} - \frac{\chi_{10}}{3}\right)^2, \quad (37)$$
$$c_1 = \pm t\left(\frac{1}{4} + \chi_{10}\right) + \frac{24t^2}{3W}\left(\frac{1}{4} - \frac{\chi_{10}}{3}\right)^2,$$

and the ground-state energy per site becomes

$$e_0 = c_0\delta + c_1\pi\delta^2 + 2J\chi_{10}. \quad (38)$$

This can now be used to search for a minimum of e_0 as a function of χ_{10}. It turns out that, for most parameter values, this expression favors a χ_{10} that is as negative as possible. We thus set $\chi_{10} = -0.33$, the value realized in the ground state of the Heisenberg antiferromagnet. This is obviously the absolute lower bound for the nearest-neighbor spin-correlation function that can be realized by any wave function.

IV. STRONG-COUPLING THEORY: LARGE FERMI SURFACE

The strong-coupling description of the phase with a large Fermi surface has been given in Refs. 50 and 51 (see, also, Ref. 56 for a different derivation) and here we sketch the derivation only roughly. We start again by defining the vacuum state for the theory, which now reads as

$$|\Psi_0\rangle = 2^{-N/2} \prod_i (c_{i,\uparrow}^\dagger d_{i,\downarrow}^\dagger - c_{i,\downarrow}^\dagger d_{i,\uparrow}^\dagger)|0\rangle. \quad (39)$$

This is a product of local singlets and is the ground state of the model for $t/W = J/W = 0$ and a hole doping of $\delta = 1$. Acting with the hopping term H_t onto (39) produces charge fluctuations, i.e., states of the type

$$c_{j,\sigma}^\dagger c_{i,\sigma} |\Psi_0\rangle. \quad (40)$$

In this state, both cells i and j have a total spin of $1/2$, which is carried by the unpaired d-hole spin. We now identify the quasiparticle states of a single unit cell i as follows:

$$|0\rangle \rightarrow \frac{1}{\sqrt{2}}(c_{i,\uparrow}^\dagger d_{i,\downarrow}^\dagger - c_{i,\downarrow}^\dagger d_{i,\uparrow}^\dagger)|0,$$
$$a_{i,\uparrow}^\dagger|0\rangle \rightarrow d_{i,\uparrow}^\dagger|0\rangle,$$
$$a_{i,\downarrow}^\dagger|0\rangle \rightarrow d_{i,\downarrow}^\dagger|0\rangle, \quad (41)$$
$$b_{i,\uparrow}^\dagger|0\rangle \rightarrow c_{i,\uparrow}^\dagger c_{i,\downarrow}^\dagger d_{i,\uparrow}^\dagger|0\rangle,$$
$$b_{i,\downarrow}^\dagger|0\rangle \rightarrow c_{i,\uparrow}^\dagger c_{i,\downarrow}^\dagger d_{i,\downarrow}^\dagger|0\rangle.$$

In this representation, the state (40) becomes

$$-\frac{1}{2} \text{sign}(\sigma) \, b_{j,\sigma}^\dagger \, a_{i,\bar{\sigma}}^\dagger |0\rangle. \quad (42)$$

Just as (39), the state (40) is an eigenstate of H_W with eigenvalue $-(N-2)\frac{3W}{4}$. To keep track of this large energy change, we ascribe an energy of $3W/4$ to each of the quasiparticles so that the representation of H_W becomes

$$H_W = \frac{3W}{4} \sum_{i,\sigma} (a_{i,\sigma}^\dagger a_{i,\sigma} + b_{i,\sigma}^\dagger b_{i,\sigma}). \quad (43)$$

The particles are created and annihilated in pairs and by subsequent application of the hopping term they also can propagate individually. The procedure to be followed then is entirely analogous as above: We consider a quasiparticle Hilbert space, the basis of which is formed by states of the type

$$\left(\prod_{\nu=1}^{N_a} a_{i_\nu,\sigma_\nu}^\dagger\right)\left(\prod_{\mu=1}^{N_b} b_{j_\mu,\sigma_\mu}^\dagger\right)|0\rangle. \quad (44)$$

As was the case for the small Fermi surface phase, we assume that the quasiparticles obey a hard-core constraint, i.e., all sites i_ν and j_μ are pairwise different from each other. The corresponding states in the Hilbert space of the physical Kondo lattice are

$$2^{-(N-N_a-N_b)/2} \, (-1)^{N_1} \left(\prod_{\nu=1}^{N_a} c_{i_\nu,\bar{\sigma}_\nu}\right)\left(\prod_{\mu=1}^{N_b} \left(-c_{i_\mu,\sigma_\mu}^\dagger\right)\right)|\Psi_0\rangle, \quad (45)$$

where

$$N_1 = \sum_{\nu=1}^{N_a} \delta_{\sigma_\nu,\downarrow}. \quad (46)$$

Again, we construct operators for the quasiparticles by demanding that the matrix elements of operators between the quasiparticle states (44) are equal to those of the physical operators between the corresponding Kondo-lattice states (45). We thus obtain the Hamiltonian (see Ref. 51 for details)

$$H = \frac{1}{2} \sum_{\mathbf{k},\sigma} \left[\left(-\epsilon_\mathbf{k} + \frac{3W}{2}\right) a_{\mathbf{k},\sigma}^\dagger a_{\mathbf{k},\sigma} + \left(\epsilon_\mathbf{k} + \frac{3W}{2}\right) b_{\mathbf{k},\sigma}^\dagger b_{\mathbf{k},\sigma}\right]$$
$$- \frac{1}{2} \sum_{\mathbf{k},\sigma} \text{sign}(\sigma) \, \epsilon_\mathbf{k} \, (b_{\mathbf{k},\sigma}^\dagger a_{-\mathbf{k},\bar{\sigma}}^\dagger + \text{H.c.}), \quad (47)$$

where $\epsilon_\mathbf{k} = 2t[\cos(k_x) + \cos(k_y)]$ denotes the dispersion relation for the conduction holes. If we assume that the density of quasiparticles is low, which will hold true in the limit of large W/t and close to $\delta = 1$, it will again be a reasonable approximation to relax the hard-core constraint. The Hamiltonian then can be diagonalized by the ansatz

$$\gamma_{\mathbf{k},1,\sigma} = u_\mathbf{k} b_{\mathbf{k},\sigma} + v_\mathbf{k} \text{sign}(\sigma) a_{-\mathbf{k},\bar{\sigma}}^\dagger,$$
$$\gamma_{\mathbf{k},2,\sigma} = -\text{sign}(\sigma) v_\mathbf{k} b_{\mathbf{k},\sigma} + u_\mathbf{k} a_{-\mathbf{k},\bar{\sigma}}^\dagger, \quad (48)$$

and, introducing $\Delta = 3W/2$, we obtain the quasiparticle dispersion

$$E_\pm(\mathbf{k}) = \frac{1}{2}\left[\epsilon_\mathbf{k} \pm \sqrt{\epsilon_\mathbf{k}^2 + \Delta^2}\right] \approx \pm\frac{3W}{4} + \frac{\epsilon_\mathbf{k}}{2} \pm \frac{\epsilon_\mathbf{k}^2}{4\Delta}, \quad (49)$$

where the second line holds in the limit $W/t \gg 1$. The operator of total hole number is given by

$$N_h = 2N + \sum_{\mathbf{k},\sigma} (b^\dagger_{\mathbf{k},\sigma} b_{\mathbf{k},\sigma} - a^\dagger_{\mathbf{k},\sigma} a_{\mathbf{k},\sigma})$$

$$= \sum_{\mathbf{k},\sigma} \sum_{\mu=1}^{2} \gamma^\dagger_{\mathbf{k},\mu,\sigma} \gamma_{\mathbf{k},\mu,\sigma}. \tag{50}$$

The first line follows from the fact that the vacuum state (39) contributes $2N$ holes, and that each holelike (electronlike) quasiparticle increases (decreases) the number of holes by one. The second line shows that the lower of the two quasiparticle bands is filled such that the Fermi surface has a volume that corresponds to conduction holes *and* localized spins, i.e., this state has a large Fermi surface. The *apparent* contribution of the localized spins to the Fermi surface can be understood as follows: At a conduction hole density of 1 per unit cell, the state resulting from the above construction has a total hole number of 2 per unit cell. At the same time, the state has an energy gap of order $3W/2$, the energy required to break two singlets. As far as the hole number and Fermi surface (or, rather, absence of a Fermi surface) are concerned, this state therefore is completely equivalent to a band insulator, provided the localized spins contribute to the total hole number. And since the quasiparticles introduced by changing δ are spin-1/2 fermions, the Fermi surface at lower conduction-hole density is the same as that of a doped band insulator and the localized spins *apparently* contribute to the Fermi surface volume. This is therefore simply the consequence of the fact that the quasiparticles are spin-1/2 fermions.

A notable feature of the above theory is that it actually incorporates the kind of broken gauge symmetry that became apparent already in the mean-field treatment: all single-cell basis states of the physical system, i.e., the states on the right-hand side of Eq. (41), are defined only up to a phase factor. The quasiparticle Hamiltonian (47) then holds true only if the phases of all states in a given unit cell are equal so that no net phase enters the Hamiltonian. However, one might choose, e.g., the phase of the states corresponding to $b^\dagger_{i,\uparrow}|0\rangle$ and $a^\dagger_{i,\downarrow}|0\rangle$ equal to unity and the phase of the singlet state corresponding to $|0\rangle$ to be $\exp(i\phi_j)$. In this case, all matrix elements in the real-space version of (47) would acquire extra phase factors. Such a phase-disordered state might be adequate to describe the Kondo lattice at temperatures lower than the Kondo temperature but higher than the coherence temperature. In the mean-field description, we had a condensate of singlets described by the constant order parameter Δ_{cd}; since the constraint of localized d holes can not be taken into account rigorously in mean-field theory, this is probably the best approximation to an array of phase-coherent Kondo singlets.

It remains to discuss the direct d-d exchange $\propto J$. In the vacuum state, the d-d exchange can promote two singlets on neighboring sites into triplets. The matrix element for this transition is $J/2$ so that second-order perturbation theory gives the correction to the energy site

$$-N \frac{z}{2} \frac{3J^2}{8W}. \tag{51}$$

This is $\propto J^2/W$ and thus much smaller than the direct d-d exchange $\propto J$ in the phase with small Fermi surface [see Eq. (32)]. This term will be even less important because this contribution occurs only if both cells are unoccupied by quasiparticles.

In addition to this contribution of the vacuum, there is also a contribution of the quasiparticles to the exchange energy because the spin of the quasiparticles is carried by the d electron. For example, we have

$$S^+_i = a^\dagger_{i,\uparrow} a_{j,\downarrow} + b^\dagger_{i,\uparrow} b_{i,\downarrow}, \tag{52}$$

which again can be verified by comparing matrix elements of the right- and left-hand sides between quasiparticle states and physical states of the Kondo lattice.

If we relax the hard-core constraint, a straightforward calculation then gives the contribution to the ground state expectation value per site from the exchange between quasiparticles of

$$\frac{\langle H_J \rangle}{N} = -3J \left[\left(\frac{1}{N} \sum_{\mathbf{k}} \gamma_{\mathbf{k}} v^2_{\mathbf{k}} f_{1,\mathbf{k}} \right)^2 + \left(\frac{1}{N} \sum_{\mathbf{k}} \gamma_{\mathbf{k}} u^2_{\mathbf{k}} f_{1,\mathbf{k}} \right)^2 \right.$$

$$\left. + 2 \left(\frac{1}{N} \sum_{\mathbf{k}} \gamma_{\mathbf{k}} u_{\mathbf{k}} v_{\mathbf{k}} f_{1,\mathbf{k}} \right)^2 \right], \tag{53}$$

where $f_{1,\mathbf{k}}$ denotes the ground-state occupation number of the lower quasiparticle band (we have assumed that the upper band is completely empty) and $\gamma_{\mathbf{k}} = \frac{1}{2}(\cos(k_x) + \cos(k_y))$. In the limit $W/t \gg 1$, we have $u_{\mathbf{k}} \to 1$, $v_{\mathbf{k}} \to \frac{\sqrt{2}\epsilon_{\mathbf{k}}}{3W}$ so that we have approximately

$$\frac{\langle H_J \rangle}{N} = -3J \left(\frac{1}{N} \sum_{\mathbf{k}} \gamma_{\mathbf{k}} f_{1,\mathbf{k}} \right)^2. \tag{54}$$

Corrections to this will be of order J/W.

Whereas the small Fermi surface theory is valid for electron densities close to $n = 1$ electron/unit cell, the large Fermi surface theory is valid for $n = 2$ electron/unit cell. In the next step, we will compute the ground-state energy as a function of the electron density.

V. PHASE TRANSITION IN STRONG COUPLING

In the preceding two sections, we have given a strong-coupling description of the two phases with large and small Fermi surface. Our main goal was to elucidate how these phases can be characterized beyond simple mean-field theory. Clearly, it would now be desirable to compare the energies of the resulting ground states and discuss a possible phase transition between the two. It should be noted from the very beginning that this will necessarily involve some rather crude approximations because the quasiparticle Hamiltonians for the two phases a formulated in terms of fermions with a hard-core constraint. The considerations in the following section thus will necessarily have a more qualitative character.

We first consider the dominant term in the Hamiltonian H_W and collect only terms $\propto W$. In the phase with the small Fermi surface, the number of quasiparticles is $N\delta$ and, since each quasiparticle contributes $-\frac{3W}{4}$ [see Eq. (37)], we have

$\langle H_W \rangle = -\frac{3N\delta W}{4} + 0(W^0)$. The vacuum for the construction of the large Fermi surface state [Eq. (39)] contributes an energy of $-N\frac{3W}{4}$. From the quasiparticle dispersion (49), we obtain a contribution of $-N(1+\delta)\frac{3W}{4} + 0(W^0)$ because the total number of quasiparticles is $N(1+\delta)$. And, finally, there is an additional constant term of $2N\frac{3W}{4}$, which comes from inverting the two a-fermion operators in the first term on the right-hand of Eq. (47), so that we obtain $\langle H_W \rangle = -\frac{3N\delta W}{4}$. To leading order in W, the two phases thus are degenerate, which is very different from the mean-field treatment. We thus consider the kinetic energy.

In discussing the kinetic energy, we encounter the problem that the phase transition necessarily occurs for a doping range where at least one of the two states with different Fermi surface volume is far from its vacuum state (these correspond to $\delta = 0$ for the small Fermi surface state and $\delta = 1$ for the large Fermi surface state), so that relaxing the respective hard-core constraint between the quasiparticles will no longer be justified. To obtain at least qualitative results, we proceed as follows: We expect that, for a finite density of quasiparticles, the hard-core constraint leads to a reduction of the total kinetic energy. For a *single-band Hubbard model,* we can study this reduction by exact diagonalization of a small cluster. More precisely, by defining the ground-state energy of a single-band Hubbard model with Coulomb repulsion U and n electrons by $E_0^{(n)}(U)$, we can compute the function

$$\alpha(n/N) = \frac{E_0^{(n)}(U=\infty)}{E_0^{(n)}(U=0)}, \quad (55)$$

where N for the time being denotes the number of sites in the cluster. This gives the reduction of the kinetic energy due to the hard-core constraint. By evaluating both energies in the same 4×4 cluster, we may expect to cancel out the shell effects, which inevitably dominate the kinetic energy of a finite cluster. In the numerical computation of $\alpha(n/N)$, we have moreover imposed the additional restriction to use only states with total spin $S = 0$.

We have performed this procedure for different forms of the kinetic energy, i.e., for different values of the hopping integrals t' and t'' to $(1,1)$-like and $(2,0)$-like neighbors.

Figure 13 then shows the resulting $\alpha(\delta)$ for different combinations of t' and t''. The respective values of t' and t'' for each combination are given in Table I. As can be seen from Fig. 13, $\alpha(\delta)$ is relatively independent on the precise form of the kinetic energy, i.e., it seems to be an almost universal function of the particle density. $\alpha(\delta)$ can be fitted quite well by a simple quadratic function, which depends on a single parameter

$$\alpha(\delta) = 1 + \lambda\delta - (1+\lambda)\delta^2, \quad (56)$$

where $\delta = n/N$. The fit gives the value $\lambda = -0.2$.

We now *assume* that the same reduction factor remains valid also for the more complicated Hamiltonians produced by the above strong-coupling theories. It should be noted that this can not be completely wrong because the values $\alpha(0) = 1$ and $\alpha(1) = 0$ are known and the function may be expected to be slowly varying near $\delta = 0$ and rapidly varying near $\delta = 1$.

We therefore evaluate the kinetic energy for different electron densities of the quasiparticles in the states with large and small Fermi surface by computing the kinetic energy in
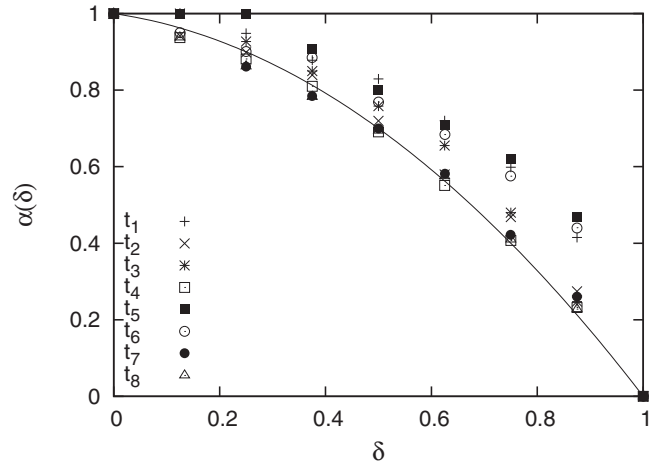
FIG. 13. The function $\alpha(\delta)$ defined in Eq. (55) evaluated numerically in a 4×4 cluster for different forms of the kinetic energy, i.e., for different values of the hopping integrals t, t', and t''. The values of the hopping integrals for the individual systems are given in Table I. The line is the function (56).

the absence of the hard-core constraint and then correcting by the factor $\alpha(\delta)$. For the large Fermi surface phase, δ is not the physical density of the conduction holes, but the density of quasiparticles

$$\tilde{\delta} = \frac{1}{N} \sum_{\mathbf{k},\sigma} (a_{\mathbf{k},\sigma}^\dagger a_{\mathbf{k},\sigma} + b_{\mathbf{k},\sigma}^\dagger b_{\mathbf{k},\sigma}). \quad (57)$$

Let us stress that it is clear from the very beginning that this procedure must lead to a level crossing for a small value δ_c of the physical hole concentration: In the absence of the correction factor $\alpha(\delta)$, the large Fermi surface phase always has a lower kinetic energy because the renormalization of the hopping integrals is much weaker in this phase [compare Eqs. (47) and (29)]. On the other hand, for $\delta \to 0$, the density of the quasiparticles $\tilde{\delta} \approx 1 - \delta$ for the large Fermi surface phase approaches 1, so that the correction factor $\alpha(\tilde{\delta})$ approaches 0, whereas the density of quasiparticles for the small Fermi surface phase is $\tilde{\delta} = \delta$ and $\alpha(\tilde{\delta})$ is close to 1. This gives a level crossing even if only the kinetic energy is taken into account and we moreover expect this level crossing to occur for small δ.

TABLE I. The values of the hopping integrals for the calculation of the renormalization of the kinetic energy in Fig. 13. The first column gives the number by which the dataset is labeled in Fig. 13.

H_t	t	t'	t''
1	1.00	0.50	0.40
2	1.00	−0.50	0.40
3	1.00	0.50	−0.40
4	1.00	−0.50	−0.40
5	1.00	2.00	2.00
6	1.00	−2.00	2.00
7	1.00	2.00	−2.00
8	1.00	−2.00	−2.00
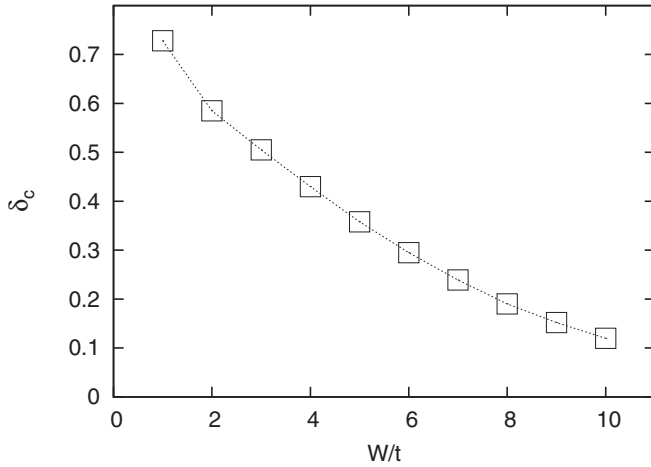
FIG. 14. Hole concentration δ_c where the phase transition from small-to-large Fermi surface occurs as a function of W/t. The small Fermi surface is realized for $\delta < \delta_c$.

Figure 14, which shows δ_c obtained by numerical calculation as a function of W/t, confirms this. δ_c decreases with increasing W/t, which can be understood as a consequence of the decrease of the bandwidth in the small Fermi surface state with increasing W/t [compare Eq. (37)].

Finally, the d-d exchange term H_J should be considered, but since we obtain a phase transition already from the kinetic energy and since the exchange energy is only a small correction for physical parameters, we restrict ourselves to a qualitative discussion. For the small Fermi surface phase, we have the contribution from the exchange energy of the localized spins amongst each other, which was $2(1 - 2\delta)J\chi_{10}$. The discussion in Sec. III suggested that χ_{10} is close to the value for the Heisenberg antiferromagnet, which is a lower bound for the nearest-neighbor spin-correlation function of localized electrons. The contribution from exchange between the quasiparticles [see Eq. (34)] is $\propto \delta^2$ and since the kinetic energy favors a level crossing at small δ (at least for larger W/t), this contribution is not important. For the large Fermi surface phase, we first have a contribution from the virtual pair creation of triplets [Eq. (51)]. Since this is of order J^2/W and will be suppressed because the density of quasiparticles is close to 1, this is not important either. Second, we have the contributions (53) or (54) from the exchange between the quasiparticles themselves, which is $\propto J$. Since there the impact of the hard-core constraint is hard to estimate, we can not definitely say which phase is favored by the Heisenberg exchange; however, this is a small correction anyway.

All in all, we thus expect a phase transition between the states with small and large Fermi surface also in the strong-coupling description. With the approximations outlined above, this transition should occur for any value of J/t, which is different from the mean-field theory where a minimum value of J/t was required. Of course, quantitative agreement between mean-field and strong-coupling theories may hardly be expected.

VI. CONCLUSION

In summary, the doping-induced transition between phases with large and small Fermi surface in the two-dimensional Kondo lattice model augmented by a Heisenberg exchange between the localized spins has been studied by mean-field and strong-coupling theories. Mean-field theory produces a phase diagram that has a rough similarity with that of cuprate superconductors: For low doping and low temperature, the localized spins do not contribute to the Fermi surface volume but form a decoupled spin liquid with pronounced singlet pairing. The spin liquid corresponds to a bond-related order parameter Δ_{dd} with $d_{x^2-y^2}$ symmetry, which describes singlet pairing between localized spins on nearest neighbors. This phase likely corresponds to the pseudogap phase in the cuprates. In mean-field theory, the Fermi surface of the conduction holes is a pocket around Γ, which is unphysical due to the absence of any coupling to the localized spins. One might conjecture, however, that the coupling to the antiferromagnetic fluctuations of the spin liquid would create hole pockets near $(\pm\frac{\pi}{2}, \pm\frac{\pi}{2})$ (see, e.g., Refs. 61 and 62) as possibly observed in ARPES.[4,7] At higher doping and low temperature, the localized spins do contribute to the Fermi surface volume and thus create a heavy fermionlike state with a large Fermi surface and an enhanced band mass. This corresponds to the overdoped regime in the cuprates and is associated with a complex on-site order parameter Δ_{cd}, which describes coherent local pairing between conduction electrons and localized spins.

At intermediate doping and low temperature, there is a phase where both order parameters coexist. This phase appears to be a $d_{x^2-y^2}$ superconductor and has a large Fermi surface with a $d_{x^2-y^2}$ gap. Superconductivity emerges because the singlet pairing between the localized spins is transferred to the mobile conduction holes by the coherent Kondo pairing. All in all, the phase diagram thus shows a certain analogy with that of the cuprates.

In mean-field theory, the superconducting transition is very different in the underdoped and overdoped regimes. Whereas in the overdoped regime we have a conventional second-order transition with a $d_{x^2-y^2}$-like gap opening on the large Fermi surface, the transition on the underdoped side corresponds to the emergence of a gapped large Fermi surface, whereas the Fermi surface takes the form of hole pockets above the transition. This may actually be consistent with experiment.[29] Mean-field theory moreover finds the transition to be first order on the underdoped side of the superconducting dome. This is, on one hand, not really expected for a superconducting transition, but on the other hand, an example of a first-order transition involving competing order parameters.[53] If the transition really were first order, an interesting possibility emerges, namely, if the surface energy between the two degenerate phases were negative (as is the case in type-II-superconductors), this would imply a tendency to form inhomogeneous states in the underdoped region.[53] In fact, one peculiar feature of underdoped cuprates is their granularity.[57–59]

One experimental feature that is not reproduced by the present theory is the opening of a gap in an apparent large Fermi surface at the pseudogap temperature as observed by Hashimoto et al.[60] In the high-temperature phase, the present mean-field theory predicts a complete decoupling of localized and conduction holes.

To further elucidate the nature of the states with different Fermi surface volume and the existence of a phase transition,

we have also performed a strong-coupling calculation. In this theory, operators that create the eigenstates of a single cell from a suitably chosen vacuum state are treated as effective fermions. The advantage of this procedure is that the Kondo coupling, which should be the largest energy scale in the problem, is treated essentially exactly due to the prediagonalization of a single cell. This theory then also yields a phase transition between states with different Fermi surface volume. As opposed to the mean-field theory, the localized and conduction holes are approximately coupled to a singlet in both phases, so that the expectation value of the Kondo exchange is the same for both phases. In the phase with small Fermi surface realized at low doping, the Kondo singlets, or Zhang-Rice singlets in the case of cuprates, form the quasiparticles so that the phase of a given Zhang-Rice singlet is determined by its momentum **k**, and it is these momenta that form the small Fermi surface. In the large Fermi surface phase, the Kondo singlets have a uniform phase and the momenta that form the Fermi surface are carried by sites with spin-1/2 and either 3 or 1 holes [whereby the density of sites with 3 holes is $\propto (W/t)^2$].

In both the mean-field and the strong coupling theories, there occurs a transition between the two states with different Fermi surface for low carrier concentration. Another complication that adds to the experimental complexity, and that has not been addressed at all in this paper, is a nematic ordering in the spin liquid plus hole pocket phase.

APPENDIX

In this Appendix, we want to address various issues related to the representation of the local singlets and triplets in terms of spin-1/2 fermion operators. We note first that, for example, the states $\hat{a}_{i,\uparrow}^{\dagger}|\Psi_0\rangle$ and $\hat{a}_{i,\downarrow}^{\dagger}|\Psi_0\rangle$ are orthogonal because their scalar product is proportional to $\langle\Psi_0|S_i^+|\Psi_0\rangle = 0$. Deviations from ideal fermion behavior appear in the overlap of states with two fermions. For example, we have

$$
\begin{aligned}
4\langle\Psi_0|\hat{a}_{i,\uparrow}\hat{a}_{j,\uparrow}\hat{a}_{j,\uparrow}^{\dagger}\hat{a}_{i,\uparrow}^{\dagger}|\Psi_0\rangle &= 1 + \tfrac{4}{3}\chi_{ij}, \\
4\langle\Psi_0|\hat{a}_{i,\uparrow}\hat{a}_{j,\downarrow}\hat{a}_{j,\downarrow}^{\dagger}\hat{a}_{i,\uparrow}^{\dagger}|\Psi_0\rangle &= 1 - \tfrac{4}{3}\chi_{ij}, \\
4\langle\Psi_0|\hat{a}_{i,\uparrow}\hat{b}_{j,1,\uparrow}\hat{b}_{j,1,\uparrow}^{\dagger}\hat{a}_{i,\uparrow}^{\dagger}|\Psi_0\rangle &= 1 + \tfrac{4}{3}\chi_{ij}, \\
4\langle\Psi_0|\hat{a}_{i,\uparrow}\hat{b}_{j,1,\downarrow}\hat{b}_{j,1,\downarrow}^{\dagger}\hat{a}_{i,\uparrow}^{\dagger}|\Psi_0\rangle &= 1 - \tfrac{4}{3}\chi_{ij}, \\
4\langle\Psi_0|\hat{a}_{i,\uparrow}\hat{b}_{j,2,\uparrow}\hat{b}_{j,2,\uparrow}^{\dagger}\hat{a}_{i,\uparrow}^{\dagger}|\Psi_0\rangle &= 1 - \tfrac{4}{3}\chi_{ij}, \\
4\langle\Psi_0|\hat{a}_{i,\uparrow}\hat{b}_{j,2,\downarrow}\hat{b}_{j,2,\downarrow}^{\dagger}\hat{a}_{i,\uparrow}^{\dagger}|\Psi_0\rangle &= 1 + \tfrac{4}{3}\chi_{ij}.
\end{aligned}
\tag{A1}
$$

The factors of 4 on the left-hand side thereby correspond to the prefactors in Eq. (24). These relations would be consistent with those for ideal Fermi operators if the spin-correlation function $\chi_{ij} = 0$. If χ_{ij} is short ranged, the local singlets and triplets thus behave like fermion operators for most distances. We expect that the same will hold true for states with more than two fermions, provided that they are pairwise more distant than the spin-correlation length ζ. This will be a reasonable assumption in the limit of low density that we are interested in. Furthermore, the neglected overlaps (being four-particle overlaps) would create an interaction between the quasiparticles rather than change their dispersion.

[1] N. E. Hussey, M. Abdel-Jawad, A. Carrington, A. P. Mackenzie, and L. Balicas, Nature (London) **425**, 814 (2003).

[2] M. Plate, J. D. F. Mottershead, I. S. Elfimov, D. C. Peets, R. Liang, D. A. Bonn, W. N. Hardy, S. Chiuzbaian, M. Falub, M. Shi, L. Patthey, and A. Damascelli, Phys. Rev. Lett. **95**, 077001 (2005).

[3] B. Vignolle, A. Carrington, R. A. Cooper, M. M. J. French, A. P. Mackenzie, C. Jaudet, D. Vignolles, Cyril Proust, and N. E. Hussey, Nature (London) **455**, 952 (2008).

[4] A. Damascelli, Z. Hussain, and Z.-X. Shen, Rev. Mod. Phys. **75**, 473 (2003).

[5] B. O. Wells, Z.-X. Shen, A. Matsuura, D. M. King, M. A. Kastner, M. Greven, and R. J. Birgeneau, Phys. Rev. Lett. **74**, 964 (1995).

[6] F. Ronning, C. Kim, D. L. Feng, D. S. Marshall, A. G. Loeser, L. L. Miller, J. N. Eckstein, I. Bozovic, and Z.-X. Shen, Science **282**, 2067 (1998).

[7] Jianqiao Meng, Guodong Liu, Wentao Zhang, Lin Zhao, Haiyun Liu, Xiaowen Jia, Daixiang Mu, Shanyu Liu, Xiaoli Dong, Wei Lu, Guiling Wang, Yong Zhou, Yong Zhu, Xiaoyang Wang, Zuyan Xu, Chuangtian Chen, and X. J. Zhou, Nature (London) **462**, 335 (2009).

[8] P. D. C. King, J. A. Rosen, W. Meevasana, A. Tamai, E. Rozbicki, R. Comin, G. Levy, D. Fournier, Y. Yoshida, H. Eisaki, K. M. Shen, N. J. C. Ingle, A. Damascelli, and F. Baumberger, Phys. Rev. Lett. **106**, 127005 (2011).

[9] X. J. Zhou, Jianqiao Meng, Yingying Peng, Junfeng He, and Li Yu, e-print arXiv:1012.3602.

[10] S. Uchida, T. Ido, H. Takagi, T. Arima, Y. Tokura, and S. Tajima, Phys. Rev. B **43**, 7942 (1991).

[11] W. J. Padilla, Y. S. Lee, M. Dumm, G. Blumberg, S. Ono, K. Segawa, S. Komiya, Y. Ando, and D. N. Basov, Phys. Rev. B **72**, 060511 (2005).

[12] N. P. Ong, Z. Z. Wang, J. Clayhold, J. M. Tarascon, L. H. Greene, and W. R. McKinnon, Phys. Rev. B **35**, 8807 (1987).

[13] H. Takagi, T. Ido, S. Ishibashi, M. Uota, S. Uchida, and Y. Tokura, Phys. Rev. B **40**, 2254 (1989).

[14] Y. Ando, Y. Kurita, S. Komiya, S. Ono, and K. Segawa, Phys. Rev. Lett. **92**, 197001 (2004).

[15] N. Doiron-Leyraud, C. Proust, D. LeBoeuf, J. Levallois, J.-B. Bonnemaison, R. Liang, D. A. Bonn, W. N. Hardy, and L. Taillefer, Nature (London) **447**, 565 (2007).

[16] S. E. Sebastian, N. Harrison, E. Palm, T. P. Murphy, C. H. Mielke, R. Liang, D. A. Bonn, W. N. Hardy, and G. G. Lonzarich, Nature (London) **454**, 200 (2008).

[17]C. Jaudet, D. Vignolles, A. Audouard, J. Levallois, D. LeBoeuf, N. Doiron-Leyraud, B. Vignolle, M. Nardone, A. Zitouni, R. Liang, D. A. Bonn, W. N. Hardy, L. Taillefer, and C. Proust, Phys. Rev. Lett. **100**, 187005 (2008).

[18]A. Audouard, C. Jaudet, D. Vignolles, R. Liang, D. A. Bonn, W. N. Hardy, L. Taillefer, and C. Proust, Phys. Rev. Lett. **103**, 157003 (2009).

[19]E. A. Yelland, J. Singleton, C. H. Mielke, N. Harrison, F. F. Balakirev, B. Dabrowski, and J. R. Cooper, Phys. Rev. Lett. **100**, 047003 (2008).

[20]A. F. Bangura, J. D. Fletcher, A. Carrington, J. Levallois, M. Nardone, B. Vignolle, P. J. Heard, N. Doiron-Leyraud, D. LeBoeuf, L. Taillefer, S. Adachi, C. Proust, and N. E. Hussey, Phys. Rev. Lett. **100**, 047004 (2008).

[21]D. LeBoeuf, N. Doiron-Leyraud, J. Levallois, R. Daou, J.-B. Bonnemaison, N. E. Hussey, L. Balicas, B. J. Ramshaw, R. Liang, D. A. Bonn, W. N. Hardy, S. Adachi, C. Proust, and L. Taillefer, Nature (London) **450**, 533 (2007).

[22]J. Chang, R. Daou, Cyril Proust, David LeBoeuf, Nicolas Doiron-Leyraud, Francis Laliberte, B. Pingault, B. J. Ramshaw, Ruixing Liang, D. A. Bonn, W. N. Hardy, H. Takagi, A. B. Antunes, I. Sheikin, K. Behnia, and Louis Taillefer, Phys. Rev. Lett. **104**, 057005 (2010).

[23]V. Hinkov, B. Keimer, A. Ivanov, P. Bourges, Y. Sidis, and C. D. Frost, e-print arXiv:1006.3278v1.

[24]M. J. Lawler, K. Fujita, Jhinhwan Lee, A. R. Schmidt, Y. Kohsaka, Chung Koo Kim, H. Eisaki, S. Uchida, J. C. Davis, J. P. Sethna, and Eun-Ah Kim, Nature (London) **466**, 347 (2010).

[25]S. E. Sebastian, N. Harrison, M. M. Altarawneh, Ruixing Liang, D. A. Bonn, W. N. Hardy, and G. G. Lonzarich, e-print arXiv:1103.4180.

[26]S. Chakravarty and H.-Y. Lee, Proc. Natl. Acad. Sci. USA **105**, 8835 (2008).

[27]D. S. Dessau, B. O. Wells, Z.-X. Shen, W. E. Spicer, A. J. Arko, R. S. List, D. B. Mitzi, and A. Kapitulnik, Phys. Rev. Lett. **66**, 2160 (1991).

[28]Y. Hwu, L. Lozzi, M. Marsi, S. La Rosa, M. Winokur, P. Davis, M. Onellion, H. Berger, F. Gozzo, F. Levy, and G. Margaritondo, Phys. Rev. Lett. **67**, 2573 (1991).

[29]Z.-X. Shen and G. A. Sawatzky, Phys. Status Solidi B **215**, 523 (1999).

[30]H. Aoki, S. Uji, A. K. Albessard, and Y. Onuki, Phys. Rev. Lett. **71**, 2110 (1993).

[31]S. K. Goh, J. Paglione, M. Sutherland, E. C. T. O. Farrell, C. Bergemann, T. A. Sayles, and M. B. Maple, Phys. Rev. Lett. **101**, 056402 (2008).

[32]Y. Onuki, R. Settai, K. Sugiyama, T. Takeuchi, T. C. Kobayashi, Y. Haga, and E. Yamamoto, J. Phys. Soc. Jpn. **73**, 769 (2004).

[33]H. Shishido, R. Settai, H. Harima, and Y. Onuki, J. Phys. Soc. Jpn. **74**, 1103 (2005).

[34]R. Settai, T. Kubo, T. D. Matsuda, Y. Haga, Y. Onuki, and H. Harima, J. Phys. Soc. Jpn. Suppl. **75**, 167 (2006).

[35]S. Doniach, Physica B (Amsterdam) **91**, 231 (1977).

[36]T. Senthil, M. Vojta, and S. Sachdev, Phys. Rev. B **69**, 035111 (2004).

[37]J. Zaanen and A. M. Oles, Phys. Rev. B **37**, 9423 (1988).

[38]R. Eder and Y. Ohta, Phys. Rev. B **51**, 6041 (1995).

[39]P. W. Leung, Phys. Rev. B **65**, 205101 (2002).

[40]P. W. Leung, Phys. Rev. B **73**, 014502 (2006).

[41]E. Dagotto and J. R. Schrieffer, Phys. Rev. B **43**, 8705 (1991).

[42]R. Eder, Y. Ohta, and T. Shimozato, Phys. Rev. B **50**, 3350 (1994).

[43]R. Eder and Y. Ohta, Phys. Rev. B **50**, 10043 (1994).

[44]S. Nishimoto, Y. Ohta, and R. Eder, Phys. Rev. B **57**, R5590 (1998).

[45]T. Tohyama, P. Horsch, and S. Maekawa, Phys. Rev. Lett. **74**, 980 (1995).

[46]R. Eder, Y. Ohta, and S. Maekawa, Phys. Rev. Lett. **74**, 5124 (1995).

[47]R. Eder and Y. Ohta, Phys. Rev. B **51**, 11683 (1995).

[48]R. Eder, K. Seki, and Y. Ohta, e-print arXiv:1101.4870.

[49]R. Eder, P. Wróbel, and Y. Ohta, Phys. Rev. B **82**, 155109 (2010).

[50]R. Eder, O. Stoica, and G. A. Sawatzky, Phys. Rev. B **55**, R6109 (1997).

[51]R. Eder, O. Rogojanu, and G. A. Sawatzky, Phys. Rev. B **58**, 7599 (1998).

[52]C.-X. Chen, H.-B. Schuttler, and A. J. Fedro, Phys. Rev. B **41**, 2581 (1990).

[53]J.-H. She, J. Zaanen, A. R. Bishop, and A. V. Balatsky, Phys. Rev. B **82**, 165128 (2010).

[54]D. L. Feng, D. H. Lu, K. M. Shen, C. Kim, H. Eisaki, A. Damascelli, R. Yoshizaki, J.-i. Shimoyama, K. Kishio, G. D. Gu, S. Oh, A. Andrus, J. O'Donnell, J. N. Eckstein, and Z.-X. Shen, Science **289**, 277 (2000).

[55]H. Ding, J. R. Engelbrecht, Z. Wang, J. C. Campuzano, S.-C. Wang, H.-B. Yang, R. Rogan, T. Takahashi, K. Kadowaki, and D. G. Hinks, Phys. Rev. Lett. **87**, 227001 (2001).

[56]S. Ostlund, Phys. Rev. B **76**, 153101 (2007).

[57]S. H. Pan, J. P. O'Neal, R. L. Badzey, C. Chamon, H. Ding, J. R. Engelbrecht, Z. Wang, H. Eisaki, S. Uchida, A. K. Gupta, K.-W. Ng, E. W. Hudson, K. M. Lang, and J. C. Davis, Nature (London) **413**, 282 (2001).

[58]K. M. Lang, V. Madhavan, J. E. Hoffman, E. W. Hudson, H. Eisaki, S. Uchida, and J. C. Davis, Nature (London) **415**, 412 (2002).

[59]A. N. Pasupathy, A. Pushp, K. K. Gomes, C. V. Parker, J. Wen, Z. Xu, G. Gu, S. Ono, Y. Ando, and A. Yazdani, Science **320**, 196 (2008).

[60]M. Hashimoto, R.-H. He, K. Tanaka, J.-P. Testaud, W. Meevasana, R. G. Moore, D. Lu, H. Yao, Y. Yoshida, H. Eisaki, T. P. Deveraux, Z. Hussain, and Z.-X. Shen, Nat. Phys. **6**, 414 (2010).

[61]R. Eder and K.W. Becker, Z. Phys. B: Condens. Matter **79**, 333 (1990).

[62]B. Lau, M. Berciu, and G. A. Sawatzky, Phys. Rev. Lett. **106**, 036401 (2011).